HAL open science

A two-dimensional method for a dispersive shallow water model

Nora Aïssiouene, Marie-Odile Bristeau, Edwige Godlewski, Anne Mangeney, Carlos Parés, Jacques Sainte-Marie

To cite this version:

Nora Aïssiouene, Marie-Odile Bristeau, Edwige Godlewski, Anne Mangeney, Carlos Parés, et al.. A two-dimensional method for a dispersive shallow water model. 2017. hal-01632522v1

HAL Id: hal-01632522

https://hal.science/hal-01632522v1

Preprint submitted on 10 Nov 2017 (v1), last revised 13 May 2020 (v5)

HAL is a multi-disciplinary open access archive for the deposit and dissemination of scientific research documents, whether they are published or not. The documents may come from teaching and research institutions in France or abroad, or from public or private research centers.

L'archive ouverte pluridisciplinaire **HAL**, est destinée au dépôt et à la diffusion de documents scientifiques de niveau recherche, publiés ou non, émanant des établissements d'enseignement et de recherche français ou étrangers, des laboratoires publics ou privés.

A two-dimensional method for a dispersive shallow water model

Nora Aissiouene, Marie-Odile Bristeau, Edwige Godlewski, Anne Mangeney, Carlos Parés, and Jacques Sainte-Marie

November 10, 2017

Contents

1 Introduction **2**

2 The model **4**
2.1 The averaged Euler system 4
2.2 The boundary conditions 5

3 Time and space discretizations **6**
3.1 Prediction - Correction scheme 6
3.2 Space discretization 7
3.3 Finite volume scheme for the prediction part 9

4 The mixed problem **9**
4.1 Compatible boundary conditions 10
4.1.1 Inflow /outflow 10
4.1.2 Slip boundary conditions 11
4.2 The variational formulation 11
4.2.1 Formulation using the shallow water divergence operator . 11
4.2.2 Formulation using the shallow water gradient operator . . 12
4.3 The inf-sup condition 13

5 Finite element approximations for the mixed problem **14**
5.1 A P1/P1 approximation 15
5.2 A P1-isoP2/P1 approximation 18

6 Numerical algorithm **21**
6.1 Iterative methods 21
6.2 Wet-dry interface 23
6.3 An improved method 24

7 Validation with analytical solutions **24**
7.1 A solitary wave 24
7.1.1 Comparison of the approximation spaces 25
7.1.2 Validation with P1-isoP2/P1 26
7.2 A periodic solution with a wet-dry interface 28

8 Application to the 2014 Iquique, Chile, earthquake **29**
8.1 Comparison with DART buoys 29

9 Conclusion **35**

Abstract

We propose a numerical method for a two-dimensional dispersive shallow water system with topography (see [15] for the derivation of the model). This model is a depth averaged Euler system and takes into account a non-hydrostatic pressure which implies to solve an incompressible system. A first approach in one dimension, based on a prediction-correction method initially introduced by Chorin-Temam (see [35]), has been presented in [1]. The prediction part leads to solving a shallow water system for which we use finite volume methods (see [5]), while the correction part leads to solving a mixed problem in velocity and pressure. From the variational formulation of the mixed problem proposed in [2], the idea is to apply a finite element method with compatible spaces to the two-dimensional problem on unstructured grids. Besides, appropriate boundary conditions are considered. In addition, to deal with the significant computational cost, an iterative method is used. Several numerical tests are performed to evaluate the efficiency of the proposed method, in particular, comparisons with analytical solutions are given and application to real tsunami case.

1 Introduction

Mathematical models for free surface flows are widely studied, however one still needs to improve the existing models as well as develop robust numerical methods. The most common way to represent the physical behavior of the free surface is to compute the solutions of the Shallow Water equations. These equations are based on a shallowness assumption and lead to assuming hydrostatic pressure. Therefore, they are used for many geophysical flows on rivers, lakes, oceans where the characteristic horizontal length is much greater than the depth. This is the case when we want to simulate the propagation of tsunamis.
However, depending on the regime of the flow, this model can be inappropriate. In particular, when the hydrostatic assumption is no longer valid, what we call dispersive effects appear and then more complex models have to be used to represent these effects. Many free surface models are available to take into consideration this dispersive effect, see [26] for the classical Green-Naghdi (GN) model and [11, 16, 20, 15] for other kinds of non hydrostatic models with bathymetry. One of the difficulties of these models arises in the development of

robust numerical methods. In this paper, we propose a new numerical scheme for a depth-averaged model derived in [15], which is based on the minimization of the energy [33]. This property provides a consistency with the Euler system [15] in terms of energy.

The non linear Shallow Water model with topograpphy is a hyperbolic system with source term, which has been studied extensively and the literature provides efficient algorithms for this model, see [25, 12] for the theory of hyperbolic systems with source term and [3, 7, 6, 4, 8] for numerical methods for the Shallow Water system with topography. Since non hydrostatic models are no longer hyperbolic, it is necessary to propose new numerical algorithms. Several approaches have been proposed to solve these kinds of models, especially in one dimension or in two dimensions with a structured grid (see [18, 11, 16, 23, 32]). A discretization with a Galerkin method has been proposed in [20] to treat the high order terms of the dispersive part, and more recently (2016), A. Duran and F. Marche performed an hybrid method [21] for the two-dimensional GN model. Indeed, there is a real need of methods to capture dispersion with a good accuracy and for real cases. In this paper, we propose a new approach dealing with a formuation without high order terms, we treat the depth-averaged Euler system developed in [15] where the non-hydrostatic pressure is an unknown of the system. The aim is to provide a robust numerical method for the two-dimensional model on an unstructured grid. The objective is to have a stable method to simulate real cases where the topography can be complex and needs an irregular mesh. Moreover, it gives the possibility to perform adaptative meshes if one wants to refine the mesh in the areas where the dispersive effects are expected. For instance, the dispersive contribution can have a significant impact on the spatio-temporal change of the water depth for the propagation of tsunamis [24],[10]. We start with the formulation proposed in , where the authors have combined a finite-volume scheme with a finite element scheme for the one dimensional non-hydrostatic model using a Chorin-Temam splitting method (initially described in [35]).

The paper is organized as follows. In the next section, we recall the depth-averaged Euler system completed with standard boundary conditions. The Section 2 is devoted to the Chorin-Temam approach (prediction-correction scheme) applied for the model problem, while in Section 4, we focus on the mixed problem which corresponds in this case to the correction part of the prediction-correction scheme. In Section 5, we propose two approximation spaces (P1/P1 and P1-isoP2/P1) for the finite element scheme applied to the mixed problem. Finally we validate the implementations using comparisons with analytical solutions, and then we give a geophysical application.

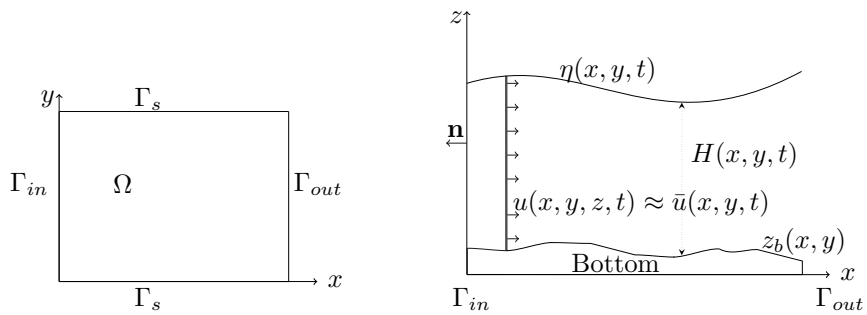

(a) View from above.

(b) Vertical cross section.

Figure 1: Model domain and notations.

2 The model

2.1 The averaged Euler system

We consider a two-dimensional domain $\Omega \subset \mathbb{R}^2$ delimited by the boundary $\Gamma = \Gamma_{in} \cup \Gamma_{out} \cup \Gamma_s$ as described in Figure 1a. We denote by $H(x,y,t)$ the water depth, $z_b(x,y)$ the topography, $\mathbf{u}(x,y,t)$ the averaged velocity of the fluid $\mathbf{u} = (u,v,w)^T$ and p the non hydrostatic pressure (see Figure 1b).

The two-dimensional depth-averaged Euler system described in [15], [36] reads:

$$\frac{\partial H}{\partial t} + \frac{\partial Hu}{\partial x} + \frac{\partial Hv}{\partial y} = 0, \tag{1}$$

$$\frac{\partial Hu}{\partial t} + \frac{\partial}{\partial x}(Hu^2) + \frac{\partial}{\partial y}(Huv) + \frac{\partial}{\partial x}(g\frac{H^2}{2} + Hp) = -(gH + 2p)\frac{\partial z_b}{\partial x}, \tag{2}$$

$$\frac{\partial Hv}{\partial t} + \frac{\partial}{\partial x}(Huv) + \frac{\partial}{\partial y}(Hv^2) + \frac{\partial}{\partial y}(g\frac{H^2}{2} + Hp) = -(gH + 2p)\frac{\partial z_b}{\partial y}, \tag{3}$$

$$\frac{\partial Hw}{\partial t} + \frac{\partial Huw}{\partial x} + \frac{\partial Hvw}{\partial y} = 2p, \tag{4}$$

completed with the incompressibility condition:

$$\frac{\partial Hu}{\partial x} + \frac{\partial Hv}{\partial y} - u\frac{\partial(H + 2z_b)}{\partial x} - v\frac{\partial(H + 2z_b)}{\partial y} + 2w = 0. \tag{5}$$

Equation (5) is obtained by an average of the free divergence condition of the Euler system.
The model (1)-(5) can be written in a more condensed form:

$$\frac{\partial H}{\partial t} + \nabla_0 \cdot (H\mathbf{u}) = 0, \tag{6}$$

$$\frac{\partial H\mathbf{u}}{\partial t} + \nabla_0 \cdot (H\mathbf{u} \otimes \mathbf{u}) + \nabla_0(\frac{g}{2}H^2) + \nabla_{sw}(p) = -gH\nabla_0(z_b), \tag{7}$$

$$\mathrm{div}_{sw}(\mathbf{u}) = 0, \tag{8}$$

where we define the operators ∇_0 and div_0 by

$$\nabla_0 f = \begin{pmatrix} \frac{\partial f}{\partial x} \\ \frac{\partial f}{\partial y} \\ 0 \end{pmatrix}, \quad \mathrm{div}_0 \mathbf{v} = \nabla_0 \cdot \mathbf{v}. \tag{9}$$

Also, we give an interpretation of the non-hydrostatic contribution by defining a shallow water version of the pressure gradient ∇_{sw} and the divergence operator div_{sw}. Assuming that f and $\mathbf{v} = (v_1, v_2, v_3)^T$ are smooth enough:

$$\nabla_{sw} f = \begin{pmatrix} H\frac{\partial f}{\partial x} + f\frac{\partial \zeta}{\partial x} \\ H\frac{\partial f}{\partial y} + f\frac{\partial \zeta}{\partial y} \\ -2f \end{pmatrix}, \tag{10}$$

$$\mathrm{div}_{sw}(\mathbf{v}) = \frac{\partial H v_1}{\partial x} + \frac{\partial H v_2}{\partial y} - v_1\frac{\partial \zeta}{\partial x} - v_2\frac{\partial \zeta}{\partial y} + 2v_3 \tag{11}$$

where we use the notation

$$\zeta = H + 2z_b. \tag{12}$$

Notice that we consider the non-hydrostatic pressure p as an unknown of the model, but we can write the total pressure p_{tot} as:

$$p_{tot} = g\frac{H}{2} + p, \tag{13}$$

where we take into account the hydrostatic pressure $g\frac{H}{2}$. An important property is that the operators div_{sw} and ∇_{sw} satisfy the duality relation

$$\int_\Omega \nabla_{sw}(f) \cdot \mathbf{v} = -\int_\Omega \mathrm{div}_{sw}(\mathbf{v}) f + \int_\Gamma H f \mathbf{v} \cdot \mathbf{n}, \tag{14}$$

where $\mathbf{n}$ is the outward unit normal vector to the boundary Γ. This property is crucial for the algorithm presented in the following since we will consider a mixed problem in velocity/pressure (see Section 4), which will lead, at the numerical level, to having an operator for the pressure and its transpose for the velocity.

2.2 The boundary conditions

The model problem (6)-(8) is completed with the following boundary conditions. Since we are considering a channel as the model domain with an inlet Γ_{in} and an outlet Γ_{out}, we impose specific conditions on each boundary. The inflow is set by imposing a given discharge $\mathbf{q_g}(x,t)$ on Γ_{in}, and a water depth $h_g(x,t)$ is

imposed on Γ_{out}. Finally, we prescribe slip boundary conditions for the velocity at the walls of the channel Γ_s:

$$\begin{aligned} H\mathbf{u}(\mathbf{x},t) &= \mathbf{q_g}(\mathbf{x},t) \quad \text{on } \Gamma_{in}, & (15)\\ H(\mathbf{x},t) &= h_g(\mathbf{x},t) \quad \text{on } \Gamma_{out}, & (16)\\ \mathbf{u}(\mathbf{x},t)\cdot\mathbf{n} &= 0 \quad \text{on } \Gamma_s. & (17) \end{aligned}$$

In most cases, we keep these boundary conditions in the numerical experiment, but we can also change the outflow boundary condition to have a free outflow by imposing a Neumann boundary condition for the elevation:

$$\nabla H \cdot \mathbf{n} = 0 \quad \text{on } \Gamma_{out}. \tag{18}$$

3 Time and space discretizations

As for the one dimensional system (see [1]), the problem (6)-(8) is solved using a Chorin-Temam splitting scheme (see [17, 35, 27, 28]). Let us recall here the general idea of the splitting scheme.

3.1 Prediction - Correction scheme

The prediction-correction method is widely used to approximate the Navier-Stokes equations and is based on a time-splitting scheme. For each time step, the problem is solved in two steps, in the first one, we use a finite-volume method to solve the hyperbolic part which is a Shallow Water system with topography (where the non hydrostatic pressure p is not evaluated). This allows us to get a first predicted state which is not divergence free. In the second step, we update the predicted state with the shallow water version of the gradient pressure evaluated in such a way that the velocity satisfies the divergence free condition (5).
Let us denote by X the vectors of unknowns:

$$X = \begin{pmatrix} H \\ Hu \\ Hv \\ Hw \end{pmatrix}$$

and $F(X)$ the matrix:

$$F(X) = \begin{pmatrix} Hu & Hv \\ Hu^2 + \frac{g}{2}H^2 & Huv \\ Huv & Hv^2 + \frac{g}{2}H^2 \\ Huw & Hvw \end{pmatrix}, \tag{19}$$

and set

$$S(X) = \begin{pmatrix} 0 \\ -gH\frac{\partial z_b}{\partial x} \\ -gH\frac{\partial z_b}{\partial y} \\ 0 \end{pmatrix} \quad \text{and} \quad R_{nh} = \begin{pmatrix} 0 \\ \nabla_{sw}(p) \end{pmatrix}. \tag{20}$$

Then, the system (6)-(8) can be written

$$\frac{\partial X}{\partial t} + \mathrm{div}_0 F(X) + R_{nh} = S(X), \tag{21}$$

$$\mathrm{div}_{sw}\,(\mathbf{u}) = 0. \tag{22}$$

We set t^0 the initial time and $t^{n+1} = t^n + \Delta t^n$ where Δt^n satisfies a stability condition (CFL) and the state X^n will denote an approximation of $X(t^n)$. For each time step, we consider an intermediate state which will be denoted with the superscript $^{n+1/2}$. So the first step leads to solving the hyperbolic system with source terms in order to get the state $X^{n+1/2} = (H^{n+1/2}, (Hu)^{n+1/2}, (Hv)^{n+1/2}, (Hw)^{n+1/2})^T$. Finally, the semi discretization in time can be summarized in the following steps:

$$X^{n+1/2} = X^n - \Delta t^n \mathrm{div}_0 F(X^n) + \Delta t S(X^n), \tag{23}$$

$$X^{n+1} = X^{n+1/2} - \Delta t^n R_{nh}^{n+1}, \tag{24}$$

$$\mathrm{div}_{sw}\,\mathbf{u}^{n+1} = 0. \tag{25}$$

Equation (24) allows us to correct the predicted value $X^{n+1/2}$ in order to obtain a state which satisfies the divergence free condition (25). The equation satisfied by the pressure is then an elliptic equation which is obtained by applying the shallow water divergence operator to the equation (24) and reads:

$$\mathrm{div}_{sw}\left(\frac{\nabla_{sw}\ p^{n+1}}{H^{n+1}}\right) = \frac{1}{\Delta t^n}\mathrm{div}_{sw}\left(\frac{(H\mathbf{u})^{n+1/2}}{H^{n+1/2}}\right). \tag{26}$$

Once the pressure has been determined by an elliptic equation (26), the correction step (24) gives the final step X^{n+1}.
In this paper, we will focus on the second step of the scheme, namely Equations (23)-(25), which we discretize by a finite element method. Therefore, we will consider the state $X^{n+1/2}$ as a given state and the state X^{n+1} as the unknown. The operator $\mathrm{div}_{sw}\left(\frac{\nabla_{sw}}{H}\right)$ is a shallow water version of the Laplacian operator and is denoted by $\triangle_{sw}$, it is written

$$\begin{aligned}\triangle_{sw}\ p &= H \triangle p + \frac{\partial p}{\partial x}\frac{\partial H}{\partial x} + \frac{\partial p}{\partial y}\frac{\partial H}{\partial y} \\ &\quad + p\left(\triangle \zeta - \frac{1}{H}\left(\left(\frac{\partial \zeta}{\partial x}\right)^2 + \left(\frac{\partial \zeta}{\partial y}\right)^2 + 4\right)\right),\end{aligned} \tag{27}$$

with ζ given by (12). The operator (27) can be written in the form of a Sturm-Liouville operator, but it is still a tricky task to study the equation (26) since it requires studying the differential term in factor of p: $\triangle\ \zeta - \frac{1}{H}\left(\left(\frac{\partial \zeta}{\partial x}\right)^2 + \left(\frac{\partial \zeta}{\partial y}\right)^2 + 4\right)$.

3.2 Space discretization

Concerning the space discretization, each step, prediction step and correction step, is solved with its own scheme. The method relies on a combination between

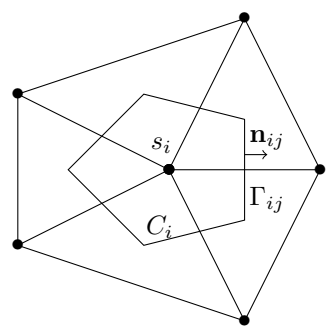

Figure 2: Representation of the dual mesh

a finite volume scheme for the hyperbolic part (23) and a finite element scheme for the elliptic part (see the correction step in Section 3.1). The idea is to start with a primal mesh which is triangular, then a dual mesh is built by the finite volume cells centered on the vertices.
Let us consider Ω the computational domain with boundary Γ, which is assumed to be polygonal. Let $\mathscr{T}$ be a triangulation of Ω. We denote by S_h the set of the vertices of the mesh:

$$S_h = \{s_i = (x_i, y_i) \in \mathscr{T}\}. \tag{28}$$

We recall here the general formalism of finite volumes on unstructured meshes, and the finite element method we use for the correction part will be detailed in Section 5.
Let us define the finite volume cell C_i associated to the vertex s_i. The cells C_i are built by joining the centers of mass of the triangles surrounding each vertex s_i. We use the following notations (see Figure 2):

- $|C_i|$, area of C_i,
- Γ_{ij}, boundary edge between the cells C_i and C_j,
- L_{ij}, length of Γ_{ij},
- $\mathbf{n}_{ij}$, unit normal to Γ_{ij}, outward to C_i ($\mathbf{n}_{ji} = -\mathbf{n}_{ij}$),
- $\mathscr{K}_i$ the set of nodes connected to the node s_i.

Remark 3.1 *The variables $H, H\mathbf{u}$ are estimated first as constant mean values on the cells C_i by the finite volume scheme, which gives the intermediate state $X^{n+1/2}$. For the finite element scheme, the state X^{n+1} is approximated at the vertices of the triangles, and for the required value of $X^{n+1/2}$ at the node s_i, we use the constant mean value computed on the cell C_i. Similarly, for the next finite volume step, the required value X^{n+1} at cell C_i is given by the*

value at node s_i. Therefore, combining the finite volume and the finite element approximations, we will denote by X_i both the constant mean value on cell C_i and the value at node s_i.

3.3 Finite volume scheme for the prediction part

We denote by X_i^n the approximation of $X(t^n)$ on a finite volume cell C_i, the state X_i^n is the approximation of the cell average of $X(t^n, \mathbf{x})$:

$$X_i^n \simeq \frac{1}{mes(C_i)} \int_{C_i} X(\mathbf{x}, t^n) d\mathbf{x}. \tag{29}$$

Then, the approximation of the prediction step (23) can be summarized as follows:

$$H_i^{n+1/2} = H_i^n - \sum_{j \in \mathscr{K}_i} \sigma_{ij} \mathcal{F}_H(H_i^n, H_j^n) - \sigma_i \mathcal{F}_H(H_i^n, H_{e,i}^n), \tag{30}$$

$$\begin{aligned}(H\mathbf{u})_i^{n+1/2} &= (H\mathbf{u})_i^n - \sum_{j \in \mathscr{K}_i} \sigma_{ij} \mathcal{F}_{(H\mathbf{u})}((H\mathbf{u})_i^n, (H\mathbf{u})_j^n) \\ &\quad - \sigma_i \mathcal{F}_{(H\mathbf{u})}((H\mathbf{u})_i^n, (H\mathbf{u})_{e,i}^n),\end{aligned} \tag{31}$$

where σ_{ij} depends on $mes(C_i)$, Δt^n and the length of the edges of cells and ensures the stability of the scheme. Similarly, $\sigma_i = \sigma_{ii}$ is computed for the boundary cells of the domain and $X_{e,i}^n$ is a fictive state associated to a cell C_i at the boundary of the domain (see [14]). The numerical fluxes $\mathcal{F}_H$ (resp. $\mathcal{F}_{(H\mathbf{u})}$) are the numerical fluxes corresponding to H (resp. $H\mathbf{u}$). We do not give details on the flux $\mathcal{F}$. For the numerical results presented in this paper, the numerical fluxes are computed by a kinetic solver with a hydrostatic reconstruction for the water depth (see [5]) but it is not the only possible choice. This ensures the well balanced property of the scheme (see [5]). In this part, the boundary conditions (15)-(17) are treated as a Riemann problem at the interface (see [14] for more details about the treatment of the boundary conditions for the Shallow Water system).

4 The mixed problem

In this section, $X^{n+1/2}$ is given following the Chorin-Temam approach, by (23) as explained in Section 3.1. We now study the mixed problem corresponding to the correction step, that is to say the system (24)-(25), and we give a variational formulation of the problem together with an appropriate treatment of the boundary conditions at the continuous level in order to be compatible with the hyperbolic part. This will make it possible to construct the finite element scheme for this problem. To do so, we consider the model domain Ω of Figure 1 with classical boundary conditions (15). The correction step consists in computing the shallow water pressure in order to satisfy the shallow water divergence

free condition (8). Notice that the water elevation is not corrected and is given by the hyperbolic part, then the equation (24) reads

$$
\begin{aligned}
H^{n+1} &= H^{n+1/2}, && (32)\\
(Hu)^{n+1} + \Delta t^n \left(H^{n+1} \frac{\partial p^{n+1}}{\partial x} + p \frac{\partial \zeta^{n+1}}{\partial x} \right) &= (Hu)^{n+1/2}, && (33)\\
(Hv)^{n+1} + \Delta t^n \left(H^{n+1} \frac{\partial p^{n+1}}{\partial y} + p \frac{\partial \zeta^{n+1}}{\partial y} \right) &= (Hv)^{n+1/2}, && (34)\\
(Hw)^{n+1} - 2\Delta t^n \, p^{n+1} &= (Hw)^{n+1/2}, && (35)
\end{aligned}
$$

completed with the divergence free condition (25) and the boundary conditions (15)-(17). From now on, we drop the superscript $^{n+1}$ and note Δt for Δt^n, thus the system (33)-(35) and (25) is written:

$$
\begin{aligned}
H\mathbf{u} + \Delta t \nabla_{sw} \, p &= H\mathbf{u}^{n+1/2}, && (36)\\
\mathrm{div}_{sw} \, (\mathbf{u}) &= 0, && (37)
\end{aligned}
$$

where H denotes the unique value $H^{n+1} = H^{n+1/2}$. This mixed problem in velocity/pressure leads to solving the pressure equation (26), and then to updating the velocity with the equation (36). Equations (36)-(37) are the "grad-div" formulation of the problem. The boundary conditions need to be detailed since they have to be consistent with the prediction part. This is the object of the next section.

4.1 Compatible boundary conditions

In geophysical models such as the Shallow Water model, it is usual to impose an inflow condition on the inlet Γ_{in}, namely $H\mathbf{u}$, and the water depth at the outflow or a free outflow, as defined by (15) and (16). At the hyperbolic level, this choice depends on the Froude number $Fr = \frac{|\mathbf{u}|}{\sqrt{gH}}$ which characterizes the flow (fluvial or torrential). In this part, we apply compatible boundary conditions on the mixed system depending on the regime chosen for the Saint-Venant problem at the prediction step. The mixed formulation will allow us to impose boundary conditions on the velocity or the pressure.

4.1.1 Inflow /outflow

Let us take the two-dimensional inflow $\mathbf{Q}_0 = ((Hu)_0^{n+1/2}, (Hv)_0^{n+1/2})^T$ which is imposed at the hyperbolic part; the vertical velocity w_0 will be treated independently. Many strategies can be applied to satisfy compatible boundary conditions. As can be seen in the equations (33)-(34), a natural choice is to keep $\mathbf{Q}_0$ the same as in the hyperbolic part, then we will impose a condition on the inlet velocity $\mathbf{u} \cdot \mathbf{n} = (u_0, v_0)^T \cdot \mathbf{n}$, with $\mathbf{n} = (n_x, n_y, 0)^T$ on Γ_{in}.
Considering the pressure equation (26) and following the same procedure detailed in [2], we can deduce that this corresponds to apply a shallow water

version of a Neumann boundary condition for the pressure:

$$\nabla_{sw}\, p \cdot \mathbf{n} = 0 \text{ on } \Gamma_{in}. \tag{38}$$

In contrast, for the outflow, we impose the water depth in the hyperbolic step and recommend a homogeneous Dirichlet boundary condition for the pressure in order to let the discharge free at the outlet, namely $p|_{\Gamma_{out}} = 0$.

4.1.2 Slip boundary conditions

For the wall of the channel represented by Γ_s in Figure 1a , we assume a slip condition for the hyperbolic part $\mathbf{u}^{n+1/2} \cdot \mathbf{n}|_{\Gamma_s} = 0$ with a Neumann boundary condition for H (see [14]) and we maintain this condition in the dispersive part, namely $\mathbf{u} \cdot \mathbf{n}|_{\Gamma_s} = 0$. Still from the pressure equation (26) and in the same spirit as in [2], we deduce that this leads to having $\nabla_{sw}\,(p) \cdot \mathbf{n}|_{\Gamma_s} = 0$. Since $\frac{\partial H}{\partial x}|_{\Gamma_s} = 0$, it gives a Neumann boundary condition for the pressure $\frac{\partial p}{\partial \mathbf{n}} = 0$ on Γ_s.

4.2 The variational formulation

First of all, we assume $\nabla\zeta \in (L^\infty(\Omega))^2$, $p_0 \in H^{-1/2}(\Gamma)$ and $H \in L^\infty(\Omega)$ is bounded below and above:

$$\alpha_1 < H < \alpha_2, \quad \alpha_1, \alpha_2 > 0. \tag{39}$$

In this section we give the variational formulation of the mixed problem (36)-(37) completed with appropriate boundary conditions:

$$\begin{aligned} \mathbf{u} \cdot \mathbf{n} &= \mathbf{u}^{n+1/2} \cdot \mathbf{n} \quad \text{on } \Gamma_{in}, && (40)\\ \mathbf{u} \cdot \mathbf{n} &= 0 \qquad\qquad \text{on } \Gamma_s, && (41)\\ p &= p_0 \qquad\qquad \text{on } \Gamma_{out}. && (42) \end{aligned}$$

In (42), to give a general formulation, we have considered a non-homogeneous Dirichlet boundary condition for the pressure. We distinguish two variational formulations using the shallow water divergence or gradient operator and we explain how to choose the most judicious one in practice.

4.2.1 Formulation using the shallow water divergence operator

In this section, we will propose a strong treatment of the boundary condition for the velocity, we introduce the spaces:

$$\begin{aligned} \mathbf{V} &= \{\mathbf{v} \in L^2(\Omega)^3,\ \mathrm{div}_{sw}\,(\mathbf{u}) \in L^2(\Omega)\} && (43)\\ \mathbf{W} &= \{\mathbf{w} \in \mathbf{V},\ \mathbf{w} \cdot \mathbf{n} = 0 \text{ on } \Gamma_{in} \cup \Gamma_s\}. && (44) \end{aligned}$$

The Hilbert space $\mathbf{W}$ is equipped with inner product $(.,.)_{\mathbf{W}}$ and induced norm $||.||_{\mathbf{W}} = ||.||_{\mathbf{L}(\Omega)^2} + ||\mathrm{div}_{sw}\,(.)||_{\mathbf{L}^2(\Omega)}$. For this variational formulation, we assume a homogeneous boundary condition for the velocity, namely, in (40) we take

$\mathbf{u}\cdot\mathbf{n}=0$ on Γ_{in}.
Then the problem (36)-(37) reads:
Find $\mathbf{u}\in\mathbf{W}$, $p\in L^2(\Omega)$ such that, $\forall\,\mathbf{v}\in\mathbf{W}$

$$\int_\Omega H\mathbf{u}\mathbf{v}\,d\mathbf{x}-\Delta t\int_\Omega \mathrm{div}_{sw}\,(\mathbf{v})\,p\,d\mathbf{x} = \int_\Omega H\mathbf{u}^{n+1/2}\cdot\mathbf{v}\,d\mathbf{x}- < H\mathbf{v}\cdot\mathbf{n}\,,p_0 >_{\Gamma_{out}}, \quad (45)$$

$$\int_\Omega \mathrm{div}_{sw}\,(\mathbf{u})q\,d\mathbf{x} = 0,\quad \forall q\in L^2(\Omega), \quad (46)$$

where we assume $p_0\in H^{-1/2}(\Gamma_{out})$ and $<\cdot,\cdot>_{\Gamma_{out}}$ represents the duality between $H^{-1/2}(\Gamma_{out})$ and $H^{1/2}(\Gamma_{out})$ and $\mathbf{u}^{n+1/2}\in\mathbf{W}$. We introduce the bilinear forms

$$a(\mathbf{u},\mathbf{v}) = \int_\Omega H\mathbf{u}\cdot\mathbf{v}d\mathbf{x},\quad \forall\mathbf{u},\mathbf{v}\in\mathbf{V} \quad (47)$$

$$b(\mathbf{v},q) = -\int_\Omega \mathrm{div}_{sw}\,(\mathbf{v})\,q\,d\mathbf{x},\quad \forall\mathbf{v}\in\mathbf{W}\,,\forall q\in L^2(\Omega). \quad (48)$$

The problem reads:
Find $\mathbf{u}\in\mathbf{W}$, $p\in L^2(\Omega)$ such that

$$a(\mathbf{u},\mathbf{v})-\Delta t\,b(\mathbf{v},p) = a(H\mathbf{u}^{n+1/2},\mathbf{v})- < H\mathbf{v}\cdot\mathbf{n}\,,p_0 >_{\Gamma_{out}},\quad \forall\mathbf{v}\in\mathbf{W}, \quad (49)$$

$$b(\mathbf{u},q) = 0,\quad \forall q\in L^2(\Omega). \quad (50)$$

To impose a non-homogeneous boundary condition on Γ_s for the velocity $\mathbf{u}$, we choose $\mathbf{u}-\bar{\mathbf{u}}_0\in\mathbf{W}$ where $\bar{\mathbf{u}}_0$ is defined on $\bar{\Omega}$ such that $\bar{\mathbf{u}}_0|_{\Gamma_s}=\bar{\mathbf{u}}^{n+1/2}|_{\Gamma_s}$.
In practice, this formulation requires to choose basis functions satisfying the slip condition in (44). Therefore, if we want to have a domain with a specific boundary, we will prefer the formulation using the shallow water gradient operator, which is described in the following.

4.2.2 Formulation using the shallow water gradient operator

We define the spaces:

$$Q = \{q\in L^2(\Omega),\nabla_{sw}\,(q)\in L^2(\Omega)^3\}, \quad (51)$$

$$Q_0 = \{q\in Q\ ,\ q|_{\Gamma_{out}}=0\}. \quad (52)$$

Using the duality relation (14), we have:

$$\int_\Omega \nabla_{sw}\,(q)\cdot\mathbf{u}\,d\mathbf{x}-\int_\Gamma qH\mathbf{u}\cdot\mathbf{n}\,ds = 0\quad \forall q\in Q,$$

then writing

$$\int_\Gamma qH\mathbf{u}\cdot n\,ds = \int_{\Gamma_{in}} qH\mathbf{u}\cdot\mathbf{n}\,ds+\int_{\Gamma_s} qH\mathbf{u}\cdot\mathbf{n}\,ds+\int_{\Gamma_{out}} qH\mathbf{u}\cdot\mathbf{n}\,ds, \quad (53)$$

and, using the boundary conditions (40)-(42), we have

$$\int_{\Gamma} qH\mathbf{u}\cdot\mathbf{n}\,ds \quad = \quad \int_{\Gamma_{in}} qH\mathbf{u}^{n+1/2}\cdot\mathbf{n}\,ds, \tag{54}$$

where the slip boundary condition is imposed in the weak form $\int_{\Gamma_s} qH\mathbf{u}\cdot\mathbf{n} = 0\ \forall q \in Q$. We apply the procedure proposed for the Navier-Stokes equations in [29]. We assume there exists $\bar{p}_0 \in Q$ a given pressure such that $p_0 = \bar{p}_0|_{\Gamma_{out}} \in H^{1/2}(\Gamma_{out})$ .Therefore, the problem (36)-(37) completed with (40)-(42) reads: Find $\tilde{p} = p - \bar{p}_0 \in Q_0$, $p \in Q$, $\mathbf{u} \in (L^2(\Omega))^3$ such that,

$$\int_{\Omega} (H\mathbf{u} + \Delta t\nabla_{sw}\tilde{p})\cdot\mathbf{v}\,d\mathbf{x} \quad = \quad \int_{\Omega} H\mathbf{u}^{n+1/2}\cdot\mathbf{v}\,d\mathbf{x} \quad \forall\mathbf{v}\in(L^2(\Omega))^3, \tag{55}$$

$$\int_{\Omega} \nabla_{sw}(q)\,\mathbf{u}\,d\mathbf{x} \quad = \quad \int_{\Gamma_{in}} qH\mathbf{u}^{n+1/2}\cdot\mathbf{n}\,ds \quad \forall q\in Q_0. \tag{56}$$

Finally, we consider the following problem:
Find $\mathbf{u} \in (L^2(\Omega))^3$, with $p \in Q$ such that, $\forall\mathbf{v} \in (L^2(\Omega))^3$,

$$\int_{\Omega} (H\mathbf{u} + \Delta t\nabla_{sw}p)\cdot\mathbf{v}\,d\mathbf{x} \quad = \quad \int_{\Omega} H\mathbf{u}^{n+1/2}\cdot\mathbf{v}\,d\mathbf{x} - \Delta t\int_{\Omega}\nabla_{sw}\bar{p}_0\cdot\mathbf{v}\,d\mathbf{x} \tag{57}$$

$$\int_{\Omega} \nabla_{sw}(q)\,\mathbf{u}\,d\mathbf{x} \quad = \quad \int_{\Gamma_{in}} qH\mathbf{u}^{n+1/2}\cdot\mathbf{n}\,ds \quad \forall q\in Q_0. \tag{58}$$

Notice that we can use the formulation with the shallow water gradient operator instead of divergence in order to avoid choosing basis functions satisfying the slip boundary condition.

The pressure equation Following the procedure of the one-dimensional problem in [2], we set $\mathbf{v} = \frac{\nabla_{sw}(q)}{H}$ and take homogeneous boundary conditions for the pressure on Γ, it leads to a variational formulation of the problem in the form:

$$(\Delta_{sw}\,p, q) \quad = \quad \frac{1}{\Delta t^n}\left(\mathrm{div}_{sw}(\mathbf{u}^{n+1/2}), q\right), \quad \forall q\in Q_{0,sw}, \tag{59}$$

where

$$Q_{sw} = \{q\in Q, |\mathrm{div}_{sw}\left(\frac{\nabla_{sw}\,q}{H}\right)\in L^2(\Omega)\},$$

$$Q_{sw} = \{q\in Q,\ \ q|_{\Gamma} = 0\}.$$

The operator Δ_{sw} is the Laplacian operator defined by (26).

4.3 The inf-sup condition

We want to establish the inf-sup condition at the continuous level to ensure the problem is well-posed. The so-called inf-sup condition was introduced by Ladyzhenskaya, Babuska and Brezzi in [9, 13, 30] to ensure the well-posedness

of mixed problems for incompressible flows and has been studied for the finite element method for instance in [22]. We consider the variational problem with Dirichlet boundary conditions for the pressure (44). The problem (49)-(50) is under the form:
Find $\mathbf{u} \in \mathbf{W}$, $p \in L^2(\Omega)$ such that

$$\begin{aligned} a(\mathbf{u},\mathbf{v}) - \Delta t\, b(\mathbf{v},p) &= a(\mathbf{f},\mathbf{v}) - < H\mathbf{v}\cdot\mathbf{n}\,, p_0 >_{\Gamma_{out}}, \quad \forall \mathbf{v} \in \mathbf{W}, & (60)\\ b(\mathbf{u},q) &= 0, \quad \forall q \in L^2(\Omega). & (61) \end{aligned}$$

where $\mathbf{f} \in \mathbf{W}$ is a given vector, $< \cdot,\cdot >_{\Gamma_{out}}$ represents the duality between $H^{-1/2}(\Gamma_{out})$ and $H^{1/2}(\Gamma_{out})$. For all $\mathbf{v} \in \mathbf{W}_0 = \{\mathbf{v} \in \mathbf{W}\,, \mathrm{div}_{sw}\,(\mathbf{v}) = 0\}$, the problem becomes:
Find $\mathbf{u} \in \mathbf{W}_0$ such that

$$a(\mathbf{u},\mathbf{v}) = a(\mathbf{f},\mathbf{v}) - < H\mathbf{v}\cdot\mathbf{n}\,, p_0 >_{\Gamma_{out}}, \quad \forall \mathbf{v} \in \mathbf{W}_0. \tag{62}$$

Under the assumption (39), it is obvious that the bilinear form a is coercive, *i.e.* for all $\mathbf{v} \in \mathbf{W}_0$:

$$a(\mathbf{v},\mathbf{v}) \geq \alpha_1 ||\mathbf{v}||^2_{L^2(\Omega)}, \;\; \alpha_1 > 0. \tag{63}$$

In addition, b is bilinear. With the assumption (39), and $q \in L^2(\Omega)$ given, if we choose $\mathbf{v} = (0,0,q)^T$, then

$$\frac{b(\mathbf{v},q)}{||q||_{L^2(\Omega)}} = 2||q||_{L^2(\Omega)}. \tag{64}$$

This implies the existence and uniqueness of the solution of (45)-(46). For the formulation with the operator ∇_{sw} , we can use a similar argument and take $\mathbf{v} = \nabla_{sw}\,(q)$.

5 Finite element approximations for the mixed problem

In this part, we apply the finite element method for the correction part (36)-(37), using the formulation with the shallow water divergence operator (45)-(46). We need two discrete spaces, one for the velocity and one for the approximation of the pressure. To satisfy the inf-sup condition for the formulation (45)-(46) , we propose two implementations, the first one is the P1/P1 and the second one is the P1-isoP2/P1 spaces. As usual, P_k denotes the space of polynomials of two variables of degree $\leq k$, and P_j/P_i denotes the pair of approximation spaces where P_j is related to the velocity and P_i is related to the pressure. For the pair P1/P1, the velocity w is approximated in the same approximation space than the pressure, and for the pair P1-isoP2/P1, the approximation space of w contains the approximation space of the pressure (see Section 5.2). For both, we give the discrete formulation and we provide a comparison of the numerical results (see Section 7.1.1) in order to choose the most accurate solution.

Choice of the formulation In practice, the choice of the formulation should be done in function of the boundary conditions. We can summarized the idea by the following:

- Unless for very specific cases, it is usual to impose a homogeneous boundary condition for the pressure since we don't know the value of the pressure in real geophysical situations, then the formulations using the gradient or the divergence shallow water operator are equivalent.
- Mainly, the choice will concern the boundary conditions for the velocity, and more precisely for $\mathbf{u}\cdot\mathbf{n}$. Using the shallow water divergence operator, it is necessary to build a discrete space with basis function satisfying slide boundary conditions. In addition, if a discharge is imposed, a lifting of the boundary condition should be applied.

In the numerical method presented below, we use the divergence shallow water formulation for which the inf-sup condition is clearly satisfied.

5.1 A P1/P1 approximation

For this first implementation, we choose a P1/P1 finite element approximation (see [34, 22]) on the primal mesh $\mathscr{T}$ introduced in 3.3, on which we approximate the variables at the nodes of the triangles (see Figure 2). We give the discrete problem with the following boundary conditions:

$$p = 0, \text{ on } \Gamma_{out} \tag{65}$$

$$\mathbf{u}\cdot\mathbf{n} = 0, \text{ on } \Gamma_s \cup \Gamma_{in} \tag{66}$$

Let us introduce the discrete spaces of approximation:

$$\begin{aligned} V_h &= \{v_h \in C_0(\Omega_h), v_h|_T \in \mathrm{P1},\ \forall\, T \in \mathscr{T}\ \}, \\ Q_h &= \{q_h \in C_0(\Omega_h), q_h|_T \in \mathrm{P1},\ \forall\, T \in \mathscr{T}\}, \end{aligned}$$

with the dimensions $\dim(Q_h) = M$, $\dim(V_h) = N$. We denote $\mathbf{V_h} = (V_h)^3$. We use a strong treatment of the boundary condition for the velocity. Therefore, we take

$$\mathbf{u}_h \in \mathbf{W_h} = \{\mathbf{v}_h \in \mathbf{V_h},\ \ \mathbf{v}_h\cdot\mathbf{n}|_{\Gamma_s} = 0\}$$

and $p_h \in Q_h$ the piecewise linear approximations of $\mathbf{u}$, p on the triangles of $\mathscr{T}$. Notice that the normal components are evaluated by mean for each boundary nodes in order to impose the slide boundary conditions $\mathbf{v}_h\cdot\mathbf{n}|_{\Gamma_s} = 0$. In addition, we assume $H_h \in V_h$, $\zeta_h \in V_h$, so we introduce:

$$p_h(\mathbf{x}) = \sum_{j\in\mathcal{J}_M} p_j\varphi_j(\mathbf{x}) \quad , \quad H_h(\mathbf{x}) = \sum_{i\in\mathcal{I}_N} H_i\varphi_i(\mathbf{x}), \tag{67}$$

$$(H\mathbf{u})_h(\mathbf{x}) = \sum_{i\in\mathcal{I}_N} (H\mathbf{u})_i\varphi_i(\mathbf{x}), \qquad \zeta_h(\mathbf{x}) = \sum_{i\in\mathcal{I}_N} \zeta_i\varphi_i, \tag{68}$$

where $\mathcal{I}_N$ (resp. $\mathcal{J}_M$) is the set of indices of the space V_h (resp. Q_h) and $\{\varphi_j\}_{j\in\mathcal{J}_M}$ (resp. $\{\varphi_i\}_{i\in\mathcal{I}_N}$) are the basis functions of Q_h (resp. V_h) and

$$\mathbf{u}_h(\mathbf{x}) = \sum_{i\in\mathcal{I}_N} \mathbf{u}_i\varphi_i(\mathbf{x}), \tag{69}$$

with

$$\mathbf{u}_i = \begin{pmatrix} u_i \\ v_i \\ w_i \end{pmatrix} = \frac{1}{H_i}\begin{pmatrix} (Hu)_i \\ (Hv)_i \\ (Hw)_i \end{pmatrix}. \tag{70}$$

We use the definitions (70) in accordance with the finite volume approximation (30)-(31) (see Remark 3.1); we will use mass lumping in the integrals to be consistent with these definitions.
The discrete formulation of problem (45)-(46) reads:
Find $\mathbf{u}_h \in \mathbf{W_h}$, $p_h \in Q_h$ such that:

$$\int_\Omega H_h\mathbf{u}_h\cdot\mathbf{v}_h\,d\mathbf{x} + \Delta t\int_\Omega \mathrm{div}_{sw}\,(\mathbf{v}_h)p_h\,d\mathbf{x} = \int_\Omega H_h\mathbf{u}_h^{n+1/2}\cdot\mathbf{v}_h\,d\mathbf{x}, \quad \forall\mathbf{v}_h\in\mathbf{W_h}, \tag{71}$$

$$\int_\Omega \mathrm{div}_{sw}\,(\mathbf{u}_h)q_h\,d\mathbf{x} = 0 \quad \forall q_h\in Q_h. \tag{72}$$

In order to describe the method, we introduce the following notations:

- $S_h = \{s_i = (x_i, y_i) \in \mathscr{T}\}$: the vertices of the triangular mesh (see (28)),
- $K_{h,i} = \{T \in \mathscr{T} | s_i \in T\}$: the triangles connected to a vertex s_i.

Using definitions (67)-(70), the equations (71)-(72) become:

$$\sum_{i\in\mathcal{I}_N}\left(\int_\Omega H_i\mathbf{u}_i\varphi_i(\mathbf{x})\cdot\mathbf{v}_h(\mathbf{x})\,dx\right) - \sum_{j\in\mathcal{J}_M}\Delta t\left(\int_\Omega \mathrm{div}_{sw}\,(\mathbf{v}_h(\mathbf{x}))\phi_j(\mathbf{x})\,d\mathbf{x}\right)p_j$$
$$= \sum_{i\in\mathcal{I}_N}\left(\int_\Omega H_i\mathbf{u}_i^{n+1/2}\varphi_i(\mathbf{x})\cdot\mathbf{v}_h(\mathbf{x})\,d\mathbf{x}\right), \quad \forall\mathbf{v}_h\in\mathbf{W_h}, \tag{73}$$

completed with the divergence free condition:

$$-\sum_{i\in\mathcal{I}_N}\left(\int_\Omega \mathrm{div}_{sw}\,(\varphi_i)\,q_h\,\mathbf{u}_i\,d\mathbf{x}\right) = 0, \quad \forall q_h\in Q_h. \tag{74}$$

We introduce the pressure vector $P = (p_j)_{1\le j\le M}$ and the velocity vector $U = \begin{pmatrix} U_1, & U_2, & U_3 \end{pmatrix}^T$, with $U_1 = (u_i)_{1\le i\le N}$, $U_2 = (v_i)_{1\le i\le N}$, and $U_3 = (w_i)_{1\le i\le N}$.
Then the problem (73)-(74) can be written as:

$$A_HU + \Delta tB^TP = A_HU^{n+1/2}, \tag{75}$$

$$BU = 0, \tag{76}$$

with the classical notations (see [34]) for the mass matrix A_H, the divergence operator matrix B. The matrix A_H depends on the water depth H and is composed of the three diagonal matrices M_H:

$$A_H = \begin{pmatrix} M_H & 0 & 0 \\ 0 & M_H & 0 \\ 0 & 0 & M_H \end{pmatrix},$$

with $M_{H\,ji}$ the approximation of $\sum_{T\in K_{h,i}} \int_T H_i \varphi_i \varphi_j d\mathbf{x}$. More precisely, using mass lumping we obtain:

$$M_{H\,ji} = \sum_{T\in K_{h,i}} \frac{mes(T)}{3} H_i \delta_{ij}. \tag{77}$$

We have denoted by B the shallow water divergence operator defined by (74):

$$B = \begin{pmatrix} B_1 & B_2 & B_3 \end{pmatrix},$$

and using the definition of the shallow water operator div_{sw} in (11), we obtain:

$$\begin{aligned}
{B^T}_{1\,ji} &= -\sum_{T\in K_{h,i}} \int_T \frac{\partial H_h \varphi_i}{\partial x} \varphi_j d\mathbf{x} + \sum_{T\in K_{h,i}} \int_T \varphi_i \varphi_j \frac{\partial \zeta_h}{\partial x} d\mathbf{x}, \\
{B^T}_{2\,ji} &= -\sum_{T\in K_{h,i}} \int_T \frac{\partial H_h \varphi_i}{\partial y} \varphi_j d\mathbf{x} + \sum_{T\in K_{h,i}} \int_T \varphi_i \varphi_j \frac{\partial \zeta_h}{\partial y} d\mathbf{x}, \\
{B^T}_{3\,ji} &= 2 \sum_{T\in K_{h,i}} \int_T \varphi_i \varphi_j d\mathbf{x}.
\end{aligned}$$

Finally, the algebraic system (75)-(76) reads:

$$\begin{pmatrix} \frac{1}{\Delta t} M_H & 0 & 0 & \tilde{B}_1 \\ 0 & \frac{1}{\Delta t} M_H & 0 & \tilde{B}_2 \\ 0 & 0 & \frac{1}{\Delta t} M_H & \tilde{B}_3 \\ \tilde{B}_1^T & \tilde{B}_2^T & \tilde{B}_3^T & 0 \end{pmatrix} \begin{pmatrix} U_1 \\ U_2 \\ U_3 \\ P \end{pmatrix} = \begin{pmatrix} \frac{1}{\Delta t} M_H & 0 & 0 \\ 0 & \frac{1}{\Delta t} M_H & 0 \\ 0 & 0 & \frac{1}{\Delta t} M_H \\ 0 & 0 & 0 \end{pmatrix} \begin{pmatrix} U_1^{n+1/2} \\ U_2^{n+1/2} \\ U_3^{n+1/2} \end{pmatrix}. \tag{78}$$

By analogy with the continuous problem, applying the matrix Bt to the equation (75), we obtain the discrete elliptic equation of the pressure:

$$B A_H^{-1} B^T P = B U^{n+1/2}, \tag{79}$$

which is the discretization of the pressure equation (59). We now give some numerical approximations of the integrals we use for each matrix. The matrix B is computed with the following formulas:

$${B_1}_{ji} = -\sum_{T\in K_{h,i}} \left.\frac{\partial H_h}{\partial x}\right|_T \int_T \varphi_i \varphi_j \, d\mathbf{x} - \sum_{T\in K_{h,i}} \left.\frac{\partial \varphi_i}{\partial x}\right|_T \int_T H_h \varphi_j \, d\mathbf{x}$$

$$
\begin{aligned}
& + \sum_{T\in K_{h,i}} \left.\frac{\partial \zeta_h}{\partial x}\right|_T \int_T \varphi_i\varphi_j \, d\mathbf{x}, \\
B_{2\,ji} &= -\sum_{T\in K_{h,i}} \left.\frac{\partial H_h}{\partial y}\right|_T \int_T \varphi_i\varphi_j \, d\mathbf{x} - \sum_{T\in K_{h,i}} \left.\frac{\partial \varphi_i}{\partial y}\right|_T \int_T H_h\varphi_j \, d\mathbf{x} \\
& + \sum_{T\in K_{h,i}} \left.\frac{\partial \zeta_h}{\partial y}\right|_T \int_T \varphi_i\varphi_j \, d\mathbf{x}, \\
B_{3\,ji} &= 2\sum_{T\in K_{h,i}} \frac{mes(T)}{3}\delta_{ij}.
\end{aligned}
$$

$$
\begin{aligned}
B_{1\,ji} &= -\sum_{T\in K_{h,i}} \left.\frac{\partial \varphi_i}{\partial x}\right|_T \int_T H_h\varphi_j \, d\mathbf{x} + 2\sum_{T\in K_{h,i}} \left.\frac{\partial z_{bh}}{\partial x}\right|_T \int_T \varphi_i\varphi_j \, d\mathbf{x}, \\
B_{2\,ji} &= -\sum_{T\in K_{h,i}} \left.\frac{\partial \varphi_i}{\partial y}\right|_T \int_T H_h\varphi_j \, d\mathbf{x} + 2\sum_{T\in K_{h,i}} \left.\frac{\partial z_{bh}}{\partial y}\right|_T \int_T \varphi_i\varphi_j \, d\mathbf{x}, \\
B_{3\,ji} &= 2\sum_{T\in K_{h,i}} \frac{mes(T)}{3}\delta_{ij}.
\end{aligned}
$$

In the first terms of $B_{1\,ji}$ and $B_{2\,ji}$, we use definition (67) of H_h with mass lumping, and we obtain the following formula:

$$
\int_T H_h\varphi_j \, dx = \sum_k \int_T H_k\varphi_k\varphi_j \, d\mathbf{x} = \int_T H_i\varphi_j \, d\mathbf{x} = \frac{mes(T)}{3} H_i. \tag{80}
$$

The projection of the shallow water divergence on a vertex of the mesh is defined by:

$$
\mathrm{div}_{sw}\,(\mathbf{u}_h)|_j = \frac{3}{Supp(\varphi_j)} \sum_{i\in\mathcal{I}_N} \int_\Omega \mathrm{div}_{sw}\,(\boldsymbol{\varphi}_i(\mathbf{x}))\varphi_j(\mathbf{x}) \, d\mathbf{x}\, \mathbf{u}_i \quad \forall \boldsymbol{\varphi}_i \in \boldsymbol{W}_h, \varphi_j \in Q_h,
$$

where $Supp(\varphi_j)$ is the area of the support of the function φ_j and is computed by: $Supp(\varphi_j) = \sum_{T\in K_{h,j}} mes(T)$.

Remark 5.1 *Notice that mass lumping is chosen for the approximation of M_H in order to be consistent at the update step:*

$$
A_H U + \Delta t B^T P = A_H U^{n+1/2},
$$

since $U^{n+1/2}$ is not written in the same approximation space in the finite volume part, it is more convenient to have a diagonal matrix in practice.

5.2 A P1-isoP2/P1 approximation

In this part, we propose another approximation by finite elements, using this time the spaces P1-iso-P2/ P2 (see [34]) in which we define a coarse triangular

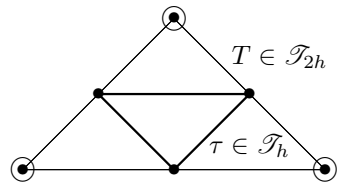

Figure 3: Representation of the triangulation. The velocity is evaluated on the black nodes, while the pressure is evaluated on the circles.

mesh $\mathscr{T}_{2h}$ and a fine mesh $\mathscr{T}_h$. The fine mesh corresponds to the primal mesh introduced for the finite volume method 3.3. Unlike the previous approximation, the velocity and the pressure are defined in two different spaces. This allows us to approximate the pressure in a smaller mesh than the velocity. Let us introduce the discrete spaces of approximation:

$$\begin{aligned} V_h &= \{v_h \in C_0(\Omega_h),\ \mathbf{v}_h|_\tau \in \mathrm{P1},\ \forall\, \tau \in \mathscr{T}_h\}, \\ Q_h &= \{q_h \in C_0(\Omega_h),\ q_h|_T \in \mathrm{P1},\ \forall\, T \in \mathscr{T}_{2h}\}, \end{aligned}$$

with the dimensions $\dim(V_h) = N$ and $\dim(Q_h) = M$. In addition, we assume $H_h \in V_h$. In practice, the triangulation $\mathscr{T}_h$ is obtained by subdividing each triangle $T \in \mathscr{T}_{2h}$ into four triangles τ by joining the middle of the edges, as shown in Figure 3. In these spaces of approximation, the velocity on the coarse mesh is evaluated with the same degree of freedom as the P2 space. Then we expect a better approximation using P1-isoP2/P1 rather than P1/P1 on the coarse mesh.
In order to describe the method, we introduce the following notations:

- $S_h = \{s_i = (x_i, y_i) \in \mathscr{T}_h\}$: the vertices of the fine mesh,
- $S_{2h} = \{s_j = (x_j, y_j) \in \mathscr{T}_{2h}\}$: the vertices of the coarse mesh,
- $K_{h,i} = \{\tau \in \mathscr{T}_h | s_i \in \tau\}$: the triangles of the fine mesh connected to node s_i,
- $K_{2h,j} = \{T \in \mathscr{T}_{2h} | s_j \in T\}$: the triangles of the coarse mesh connected to node s_j.

We take $\mathbf{u}_h \in \mathbf{W_h}$ and $p_h \in Q_h$, with $\mathbf{W_h} = \{\mathbf{v}_h \in \mathbf{V_h},\ \ \mathbf{v}_h \cdot \mathbf{n}|_{\Gamma_s} = 0\}$.

$$p_h(\mathbf{x}) = \sum_{j \in \mathcal{J}_M} p_i \phi_j(\mathbf{x}) \quad , \quad H_h = \sum_{i \in \mathcal{I}_N} H_i \varphi_i(\mathbf{x}) \quad , \quad (H\mathbf{u})_h = \sum_{i \in \mathcal{I}_N} (H\mathbf{u})_i \varphi_i(\mathbf{x}),$$

where ϕ_j (resp. φ_i) are the basis functions of Q_h (resp. V_h) and

$$\mathbf{u}_h(\mathbf{x}) = \sum_{i \in \mathcal{I}_N} \mathbf{u}_i \varphi_i(\mathbf{x}),$$

with $\mathbf{u}_i$ defined as in (69). Then matrix $\tilde{B}^T$ is computed with the following approximation

$$
\begin{aligned}
{B^T}_{1\,ji} &= -\sum_{T\in K_{2h,i}} \frac{\partial \phi_j}{\partial x}\bigg|_T \sum_{\tau\in T}\int_\tau H_h\varphi_i\, d\mathbf{x} - \sum_{T\in K_{2h,i}} \frac{\partial H_h}{\partial x}\bigg|_T \sum_{\tau\in T}\int_\tau \phi_j\varphi_i\, d\mathbf{x} \\
&\quad + \sum_{T\in K_{2h,i}}\sum_{\tau\in T} \frac{\partial \zeta_h}{\partial x}\bigg|_\tau \int_\tau \varphi_i\phi_j\, d\mathbf{x}, \\
{B^T}_{2\,ji} &= -\sum_{T\in K_{2h,i}} \frac{\partial \phi_j}{\partial y}\bigg|_T \sum_{\tau\in T}\int_\tau H_h\varphi_i\, d\mathbf{x} - \sum_{T\in K_{2h,i}} \frac{\partial H_h}{\partial y}\bigg|_T \sum_{\tau\in T}\int_\tau \phi_j\varphi_i\, d\mathbf{x} \\
&\quad + \sum_{T\in K_{2h,i}}\sum_{\tau\in T} \frac{\partial \zeta_h}{\partial y}\bigg|_\tau \int_\tau \varphi_i\phi_j\, d\mathbf{x}, \\
{B^T}_{3\,ji} &= 2\sum_{T\in K_{2h,i}}\sum_{\tau\in T}\int_\tau \varphi_i\phi_j d\mathbf{x}.
\end{aligned}
$$

$$
\begin{aligned}
{B^T}_{1\,ji} &= -\sum_{T\in K_{2h,i}} \frac{\partial H_h}{\partial x}\bigg|_T \sum_{\tau\in T}\int_\tau \phi_j\varphi_i\, d\mathbf{x} + \sum_{T\in K_{2h,i}}\sum_{\tau\in T} \frac{\partial z_{bh}}{\partial x}\bigg|_\tau \int_\tau \varphi_i\phi_j\, d\mathbf{x}, \\
{B^T}_{2\,ji} &= -\sum_{T\in K_{2h,i}} \frac{\partial H_h}{\partial y}\bigg|_T \sum_{\tau\in T}\int_\tau \phi_j\varphi_i\, d\mathbf{x} + \sum_{T\in K_{2h,i}}\sum_{\tau\in T} \frac{\partial z_{bh}}{\partial y}\bigg|_\tau \int_\tau \varphi_i\phi_j\, d\mathbf{x}, \\
{B^T}_{3\,ji} &= 2\sum_{T\in K_{2h,i}}\sum_{\tau\in T}\int_\tau \varphi_i\phi_j d\mathbf{x}.
\end{aligned}
$$

As for (80), we choose H_h and z_{bh} linear on each triangle $\tau \in \mathscr{T}_h$ and we use mass lumping:

$$\int_\tau H_h\varphi_i d\mathbf{x} = H_i\frac{mes(\tau)}{3}$$

and

$$\int_\tau \varphi_i\phi_j d\mathbf{x} = \frac{mes(\tau)}{3}\sum_{\mathbf{x}\in\bar{s}(\tau)} \varphi_i(\mathbf{x})\phi_j(\mathbf{x}),$$

where $s(\tau) = \{v_0, v_1, v_2\}$ are the three vertices of the triangle τ. Finally, the discrete version of the shallow water divergence operator is defined for each vertex of the coarse mesh by:

$$\mathrm{div}_{sw}\,\mathbf{u}_j = \frac{3}{Supp(\phi_j)}\sum_{i\in\mathcal{I}_N}\int_\Omega \nabla_{sw}\,\phi_j\cdot\varphi_i\, d\mathbf{x}\,\mathbf{u}_i. \tag{81}$$

This definition is used numerically and can be seen as a diagonal preconditioner to solve Equation (79).

6 Numerical algorithm

In this section, we give details on the algorithm we use to combine the finite volume method and the finite element method in practice. For the sake of clarity, we just give an overview of the steps of the algorithm. Assuming we know $H^n, H\mathbf{u}^n$, the combined finite volume/finite element method (23)-(25) can be summarized by the following steps:

- Solve the hyperbolic part (23) with the finite volume scheme (30)-(31) and get $(H^{n+1/2}, H\mathbf{u}^{n+1/2})$. Because of equation (32), we obtain H^{n+1} as well.
- Solve the elliptic problem (79) to obtain p^{n+1}. We use the iterative method described below.
- Update the velocity $\mathbf{u}^{n+1}$ in the correction step (75) using $\nabla_{sw}\, p^{n+1}$.

6.1 Iterative methods

Whenever possible, the linear problem (75)-(76) leading to (79), is solved in practice with iterative methods. Several algorithms allow us to solve the classical mixed problem (36)-(37) in the grad-div form. This is usually applied to the finite element method for the Navier-Stokes equations, see [34, 29]. We describe here the Conjugate Gradient method and the Uzawa algorithm (see [31, 34]) which uses the duality between the operators. In practice, to take the boundary conditions into account, the matrix is built in two blocks in which one part contains the elements of $\tilde{B}^T A_H^{-1} \tilde{B}$ for all the nodes that have to be solved and another diagonal part which is the Identity and corresponds to impose Dirichlet conditions for the pressure. Then the contribution of matrix $\tilde{B}$ associated with the given pressure is affected on the right hand side. The matrix problem can be written:

$$\begin{pmatrix} \mathcal{A} & 0 \\ 0 & Id \end{pmatrix} P = \begin{pmatrix} \frac{1}{\Delta t}\mathcal{D} - (\mathcal{A}_G) P_G \\ P_G \end{pmatrix}, \tag{82}$$

where $\mathcal{A}$ is the matrix extracted from $\tilde{B}^T A_H^{-1} \tilde{B}$ corresponding to the fact that we restrict to the nodes of unknowns, $\mathcal{A}_G$ to the nodes of the given pressure P_G respectively. The matrix $\mathcal{D}$ is the shallow water divergence vector of the unknown nodes at the prediction part. This reduces the size of the problem and allows us to apply the Conjugate Gradient algorithm. The initialization is done with the state $(Hu, Hv, Hw)^{n+1/2}$ computed at the hyperbolic step. For the sake of clarity, we drop the superscripts $^{n+1/2}$ and we denote with the superscript $^{(k)}$ the index iteration of the iterative method. In addition, we use the notation: $f = \frac{1}{\Delta t}\mathcal{D} - \mathcal{A}_G P_G$. Then the CG algorithm can be summarized as:
Initialization:

$$r^{(0)} \quad = \quad f - \mathcal{A} P^{(0)},$$

$$d^{(0)} = -r^{(0)}.$$

For $k > 0$

$$\begin{aligned}
\rho &= \frac{(r^{(k)}, d^{(k)})}{(d, \mathcal{A}d^{(k)})}, \\
P^{(k+1)} &= P^{(k)} + \rho d^{[k)}, \\
r^{(k+1)} &= r^{(k)} + \rho \mathcal{A} d^{(k)}, \\
\gamma^{(k)} &= \frac{||r^{k+1}||^2}{||r^k||^2}, \\
d^{(k+1)} &= -r^{(k)} + \gamma^{(k)} d^{(k)}.
\end{aligned}$$

Then, the correction is applied to the velocity.
For the description of the Uzawa problem, let us now use the duality between the operators (26) and (11), keeping the notations

$$\begin{aligned}
&U^{(0)}, P^{(0)} given, \\
A_H U^{(k+1)} &= A_H U^{n+1/2} - \Delta t \tilde{B} P^{(k+1)}, \\
P^{(k+1)} &= P^{(k)} + \alpha \tilde{B}^T U^{(k)},
\end{aligned}$$

with α chosen such that $0 < \alpha < \frac{2}{\max \lambda_i}$ with λ_i the eigenvalues of $BA_H^{-1}B^T$.
The CG algorithm adapted for problem (75)-(76) in the form of the Uzawa algorithm reads:
Initialization:

$$U^0 = U^{n+1/2},$$
$$d^{(0)} = -r^{(0)} = \tilde{B}^T U^{(0)},$$

$k > 0$:

$$\alpha^k = \frac{(r^{(k)}, d^k)}{(\tilde{B} d^k, A_H^{-1} \tilde{B} d^k)},$$

$$\begin{aligned}
P^{(k+1)} &= P^{(k)} + \alpha^k d^{(k)}, \\
Z &= A_H U^{(k)} - \Delta t \tilde{B} P^{(k+1)}.
\end{aligned}$$

Solve the system $A_H U^{(k+1)} = Z$ (We recall that the matrix A_H is diagonal since we have used mass lumping).
Compute $\tilde{B}^T U$:

$$r^{(k+1)} = \tilde{B}^T U^{(k+1)},$$

$$\gamma^{(k)} = \frac{||r^{(k+1)}||^2}{||r^{(k)}||^2},$$
$$d^{(k+1)} = r^{(k)} + \gamma^{(k)} d^{(k)}.$$

In accordance with Equation (81) and Equation (81), the norm $||.||$ used in the iterative algorithms above take into account the normalization of the operators.

6.2 Wet-dry interface

As one can see, the method presented above only applies for non-negative water depth. The main problem comes from the shallow water equation of the pressure (26), which requires dividing the shallow water gradient by H. At the discrete level, this difficulty arises in the mass matrix (77). Yet, in the geophysical context, it is necessary to allow a dry/wet transition to model, for instance, a propagation over obstacles like islands or a wave reaching a coast line. In practice, we set the pressure p to zero when H tends to zero. This can be viewed as a Dirichlet condition on the dry zone of the domain, such that the pressure equation is solved only on the wet domain. In the iterative solver, this leads to testing the value of the water depth for each node s_j of the mesh (or for the coarse mesh if the P1-isoP2/P1 approximation is used). However, in order to avoid selecting a list of dry nodes at each time step, which would require significant computation time, we solve the whole problem and we introduce a threshold

$$\epsilon << 1, \tag{83}$$

under which the water depth is redefined by ϵ, namely $H_\epsilon = \max(H, \epsilon)$. Since the mass matrix M_H is weighted with H and needs to be inverted in the correction step, to avoid having singularities, the matrix is redefined with respect of H_ϵ as

$$M_{H_\epsilon ji} = \sum_{T \in K_{h,i}} \int_T H_\epsilon \varphi_i \varphi_j d\mathbf{x}.$$

Then, at the correction step, the shallow water gradient is redefined by

$$\nabla^\epsilon_{sw}(p)|_i = \frac{1}{Supp(\varphi_i)} \sum_j \int_\Omega \nabla_{sw}(\varphi_j) \cdot \boldsymbol{\varphi}_i d\mathbf{x}\, p_j \mathbb{1}_{H_i > H_\epsilon}, \tag{84}$$

so the velocity is not updated at these nodes by step (24). In equation (84), the function φ_j is replaced by ϕ_j if we use P1-isoP2 /P1 space approximation. Notice that introducing H_ϵ does not change the result since it appears only in the terms of degree zero for the derivative of the pressure. It only prevents us from redefining wet/dry zones at each iteration. With these definitions, the Laplacian operator written in (27) becomes:

$$\begin{aligned}
\triangle^\epsilon_{sw}(p) &= \mathrm{div}_{sw}\left(\frac{\nabla_{sw}}{H_\epsilon}\right), && (85)\\
&= H \triangle (p) + \frac{\partial p}{\partial x}\left(\frac{\partial H}{\partial x}\right) + \frac{\partial p}{\partial y}\left(\frac{\partial H}{\partial y}\right), && (86)\\
&\quad + p\left(\triangle \zeta - \frac{1}{H_\epsilon}\left(\left(\frac{\partial \zeta}{\partial x}\right)^2 + \left(\frac{\partial \zeta}{\partial y}\right)^2 + 4\right)\right). && (87)
\end{aligned}$$

6.3 An improved method

The numerical methods presented in the previous sections can be improved if we apply a Heun scheme, which is based on a Runge-Kutta method, to the Saint-Venant model and the correction part. This improvement has been detailed for the one-dimenional problem in Chapter **??** and can be straightforwardly applied to the two-dimensional case. The Heun scheme is slightly modified so that the stability (CFL) condition remains valid. For this system, our scheme is second order accurate in time and, if we use a reconstruction algorithm (see [5]) in the hyperbolic step, it is formally second order accurate in space (see [5]). However, with the correction step, the resulting scheme is no longer of order two, but introducing the Heun scheme and the reconstruction in the hyperbolic step can improve the global accuracy of the scheme. This will be illustrated in the next section.

7 Validation with analytical solutions

In this part, we propose a validation of the method using a comparison of the numerical results for two non-stationary analytical solutions.

7.1 A solitary wave

The solitary wave is a one-dimensional non-stationary analytical solution of the model. This solution has been proposed to validate the one-dimensional model in [1] and has the form:

$$\begin{aligned}
H &= H_0 + a\left(\mathrm{sech}\left(\frac{x-c_0t}{l}\right)\right)^2, \\
u &= c_0\left(1-\frac{d}{H}\right), \\
w &= -\frac{ac_0d}{lH}\mathrm{sech}\left(\frac{x-c_0t}{l}\right)\mathrm{sech}'\left(\frac{x-c_0t}{l}\right), \\
p &= \frac{ac_0^2d^2}{2l^2H^2}\left((2H_0-H)\left(\mathrm{sech}'\left(\frac{x-c_0t}{l}\right)\right)^2,\right. \\
&+ \left. H\mathrm{sech}\left(\frac{x-c_0t}{l}\right)\mathrm{sech}''\left(\frac{x-c_0t}{l}\right)\right),
\end{aligned}$$

with $d, a, H_0 \in \mathbb{R}$, $H_0 > 0$, $a > 0$ and $c_0 = \frac{l}{d}\sqrt{\frac{gH^3}{l^2-H_0^2}}$, $l = \sqrt{\frac{H_0^3}{a} + H_0^2}$.
This analytical solution is extended to two dimensions in a rectangular channel and we add $v = 0$ in the equations.
We consider a channel of dimension 30 m $\times$1 m, the water elevation H_0 is set to 1 m with significant wave amplitude $a = 0.35$m and $d = 1$m. On the model domain in Figure 1a, we set a slip boundary condition for Γ_s, a given

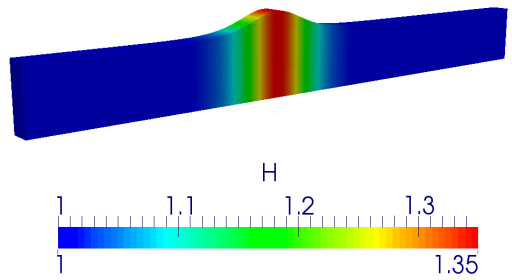

(a) Computed water depth.

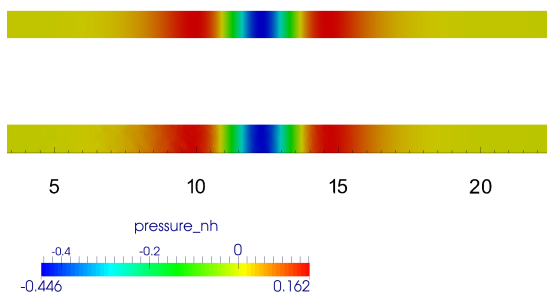

(b) non hydrostatic pressure: Analytical field at the top, numerical field at the bottom.

Figure 4: Illustration of the solitary wave propagation at $t = 1.99s$.

discharge for the inlet (15) and a water elevation at the outlet (16) with a homogeneous Dirichlet boundary condition for the pressure at the correction step. The test case is initialized with the analytical solution in the domain and we observe the propagation of the wave over time. In Figure 4, we show the computed water depth (4a) and the computed and analytical pressures (4b). This has been obtained with the P1-isoP2/P1 approximation and the wave covered approximately one wavelength.

7.1.1 Comparison of the approximation spaces

A numerical comparison of the P1/P1 and P1-isoP2/P1 approximations is proposed in order to choose the most accurate one for practical applications. In Figure 5, we compare the numerical solutions, computing the P1/P1 solution

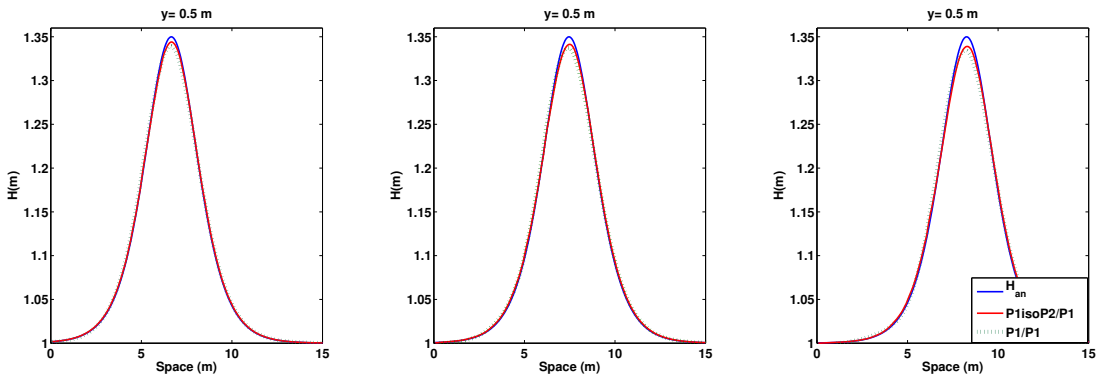

(a) H at time t=0.444213 s (b) H at time t=0.665963 s (c) H at time t=0.888782 s

Figure 5: Comparision between the P1isoP2/1 and the P1P1 approximation on the solitary wave propagation

on the fine mesh of the P1-isoP2/P1, here an unstructured mesh of 7277 nodes. After a short time, the P1/P1 method provides a less accurate solution than the P1-isoP2/P1 approximation, since we observe the amplitude of the wave obtained by the P1-isoP21/P1 method is closer to the analytical solution than the P1/P1 approximation. Notice that the discrete inf-sup condition is satisfied by the pair P1-isoP21/P1 but it is not proved for the pair P1/P1. This could explained the better accuracy obtained using P1-isoP21/P1 approximation.

7.1.2 Validation with P1-isoP2/P1

As the comparison gives better results with the P1-isoP2 / P1 spaces, we opt for this approximation to validate the method. We apply the "improved" method presented in 6.3 and obtain a good approximation of the soliton all over the propagation (see Figure 6). In Figure 6, we observe that the solitary wave conserves its amplitude over the time. The simulation shown in Figure 6 was computed with 251330 nodes for the fine mesh. We study the convergence rate of the computed solutions, computing the L^2 error at time $t = 1.99s$ for different meshes of triangle's mean edges of $h_0 = 0.0493528\,m$, $h_1 = 0.0250468\,m$ and $h_2 = 0.016781\,m$. Figure 7 shows the logarithm of the error L^2 between the analytical solution and the numerical solution in function of $\log\left(\frac{h_0}{h}\right)$ where $h = h_i, i = 0, 1, 2$. We observe a convergence rate close to 1 for the first order method, while with the improved scheme we still obtain approximately a first order convergence rate, although the error computed is smaller.

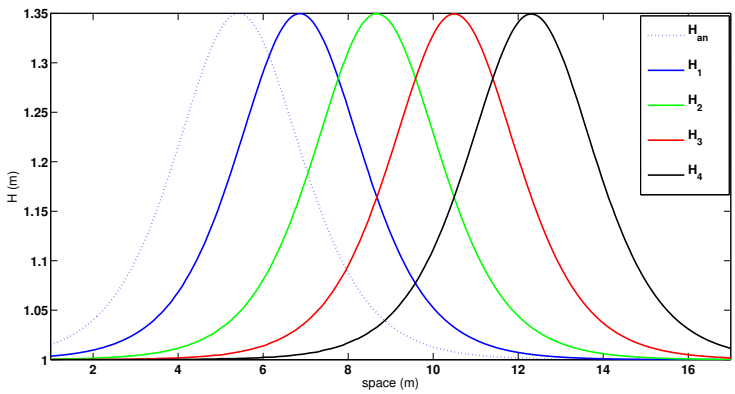

Figure 6: Cross section at the center of the channel $y = 0.5$ m; water depth of the analytical solution at initial time $H_0 = H_{an}$ and computed solution for $H_i, i = 1, ..., 4$ with $t_0 = 0\,s$, $t_1 = 0.499805\,s$, $t_2 = 0.999871\,s$, $t_3 = 1.49983\,s$, $t_4 = 1.99993\,s$ for the P1-isoP2/P1 approximation for the improved method (Heun scheme).

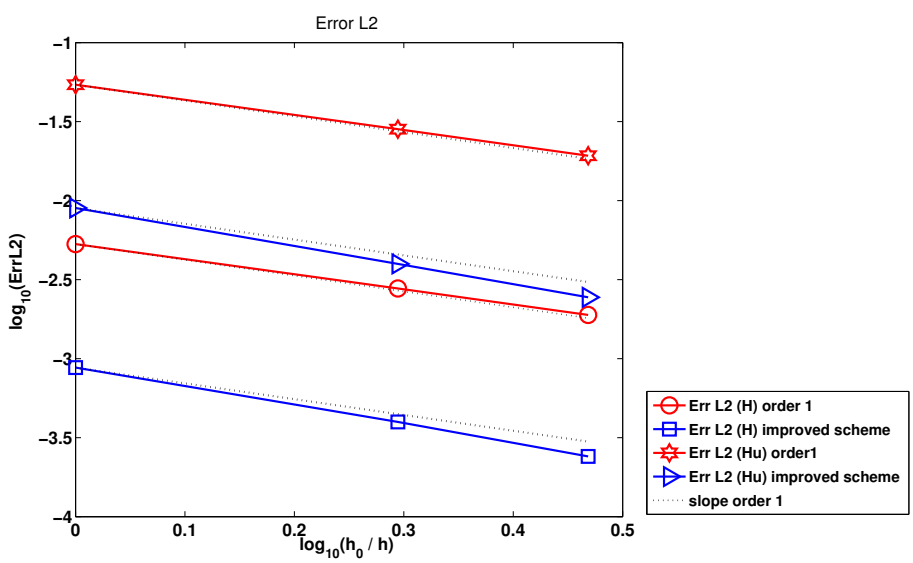

Figure 7: Convergence rate for the P1-isoP2/P1 approximation for the classical scheme (order 1 in time and space) and the improved method (Heun scheme and reconstruction in the prediction step). The L^2 is computed at time $t = 1.99s$

7.2 A periodic solution with a wet-dry interface

In this section the objective is to validate the method with a non stationary analytical solution where the free surface oscillates over the time. Such solutions have been introduced by Thacker in [37] for the Shallow Water equations and can be obtained over a paraboloid topography with a velocity (u, v) varying with respect to time. To obtain this kind of solution for the non hydrostatic model (6)-(8), we slightly modify this model by adding a given source term $s(x, y, t)$ in the third equation of the system (7), which becomes

$$\frac{\partial Hw}{\partial t} + \frac{\partial Huw}{\partial x} + \frac{\partial Hvw}{\partial y} - 2p = Hs.$$

Then an analytical solution of this modified system can be written under the form

$$\begin{aligned}
H(x,y,t) &= \max(0, H_0 - \frac{\alpha}{2}\left(x - a\cos(\sqrt{r}t)\right)^2 - \frac{\beta}{2}\left(y - a\sin(\sqrt{r}t)\right)^2), \\
u(x,y,t) &= -a\sqrt{r}\sin(\sqrt{r}t), \\
v(x,y,t) &= a\sqrt{r}\cos(\sqrt{r}t), \\
w(x,y,t) &= -\alpha a\sqrt{r}\sin(\sqrt{r}t)x + \alpha a\sqrt{r}\cos(\sqrt{r}t)y, \\
p(x,y,t) &= \frac{a^2\alpha r}{2}H, \\
s(x,y,t) &= \alpha ar\sin(\sqrt{r}t)x - \alpha ar\cos(\sqrt{r}t)y, \\
z_b(x,y) &= \frac{\alpha}{2}(x^2 + y^2),
\end{aligned}$$

where $a, \alpha > 0$ with $a\alpha < 1$, and

$$r = \frac{\alpha g}{1 - \alpha^2 a^2}.$$

We run this test on a disc domain centered in $(x, y) = (0, 0)$ with a radius of $5\,m$, with $\alpha = 0.3\,m^{-1}$, $a = 1.6\,m$ and $H_0 = 1.0\,m$ as shown in Figure 8. This case is simulated with 440746 nodes for the fine mesh (and 110588 for the coarse mesh). We use the strategy proposed in Section 6.2 to treat the wet-dry front with ϵ defined by (83) set to 10^{-5} and impose a discharge equal to zero at the boundary conditions (15) and a Dirichlet boundary condition for the pressure on Γ. In Figure 8, the representation of the free surface oscillating in the bowl is shown for different time steps. The Figure 9 presents the profile of the elevation for $y = 0$ at different time steps compared with the analytical solution. This is a crucial test case for the validation of the method since we test the dry/wet - wet/dry transitions and strong variation of the free surface. We also compute the convergence rate with the same formula described for the solitary case 7.1.2 for different meshes where $h_0 = 0.0551138\,m$, $h_1 = 0.0412458\,m$, $h_2 = 0330043\,m$, $h_3 = 0.0274674\,m$, with $h_, i = 0, ..., 3$ are the mean edges of the meshes. In Figure 10 and 11 we observe the convergence rate is close to one for the water depth, the velocity hw and the non-hydrostatic pressure p.

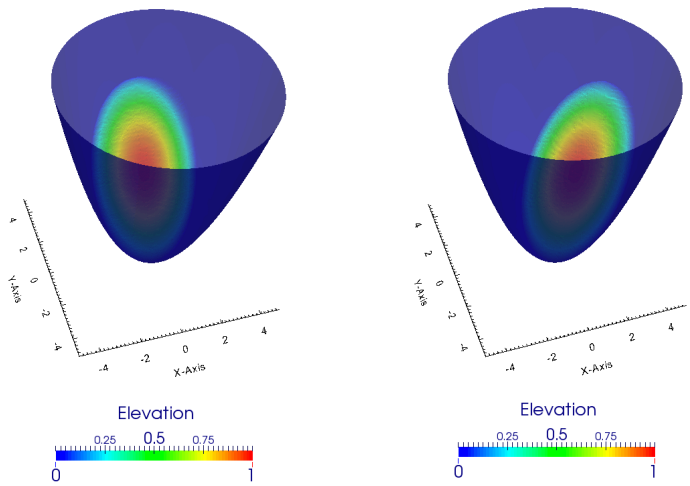

Figure 8: Simulation of the free surface oscillations in a paraboloid at different time steps.

These simulated results are computed with the improved method described in (6.3) and as expected, we obtain a similar slope for Hw and p and a better convergence for H which is not corrected in the second step of the scheme 24.

8 Application to the 2014 Iquique, Chile, earthquake

8.1 Comparison with DART buoys

In this section we apply the depth-averaged model (6)-(8) on a real geophysical application, i. e. an earthquake-generated tsunami. On April 1, 2014 at 23:46:47 UTC, a 8.2 magnitude earthquake struck off the coast of northern Chile and generated a tsunami. The earthquake was localized at 95km NW of Iquique and the elevation of the water depth has been recorded by the Deep-ocean Assessment and Reporting of Tsunamis (DART) buoys of the NOAA center for tsunami research. The objective of this part is to confront the shallow water models both hydrostatic and non-hydrostatic to the data measurements given by the DART. To do so, we use a topography given by the NOAA and a source of the earthquake given by the displacement of the topography. This source has been obtained from joined inversion of seismic [38], GPS and tsunami data (Martin Vallé, personnal communication). The comparisons are studied for two DART buoys (see Figure 12b):

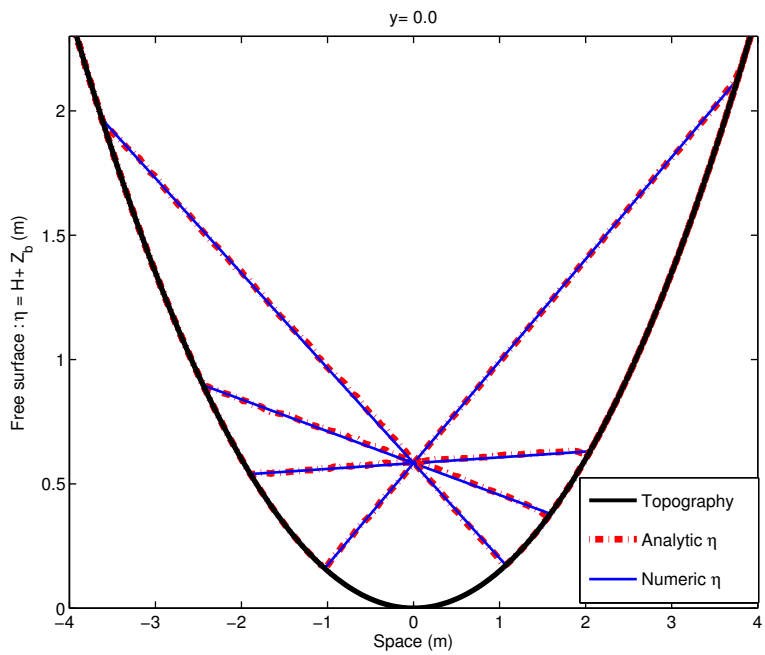

Figure 9: Cross section of the solution at $y = 0$ of the free surface $H + z_b$ compared with the analytical solution at different times: $t_0 = 0.277222\,s,\ t_1 = 0.431123\,s,\ t_2 = 0.739382\,s,\ t_3 = 0.893419\,s,\ t_4 = 1.20134\,s$

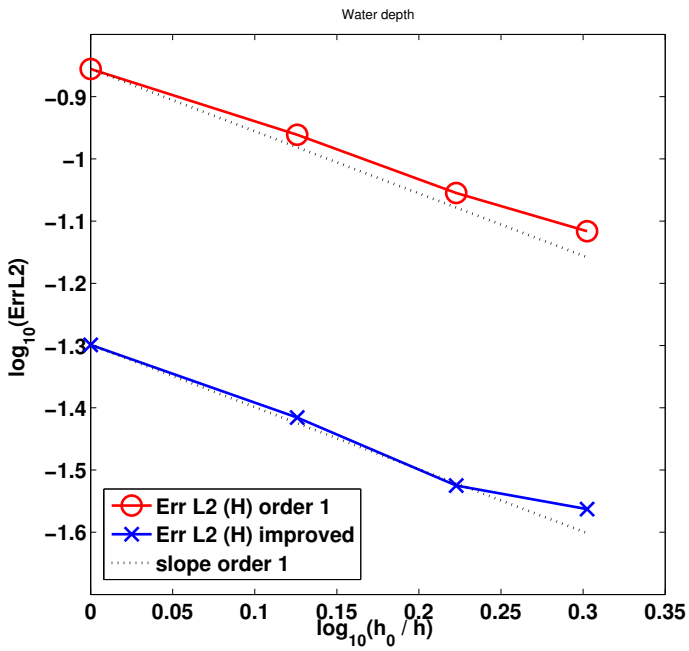

Figure 10: Convergence rate of the water depth, and the pressure

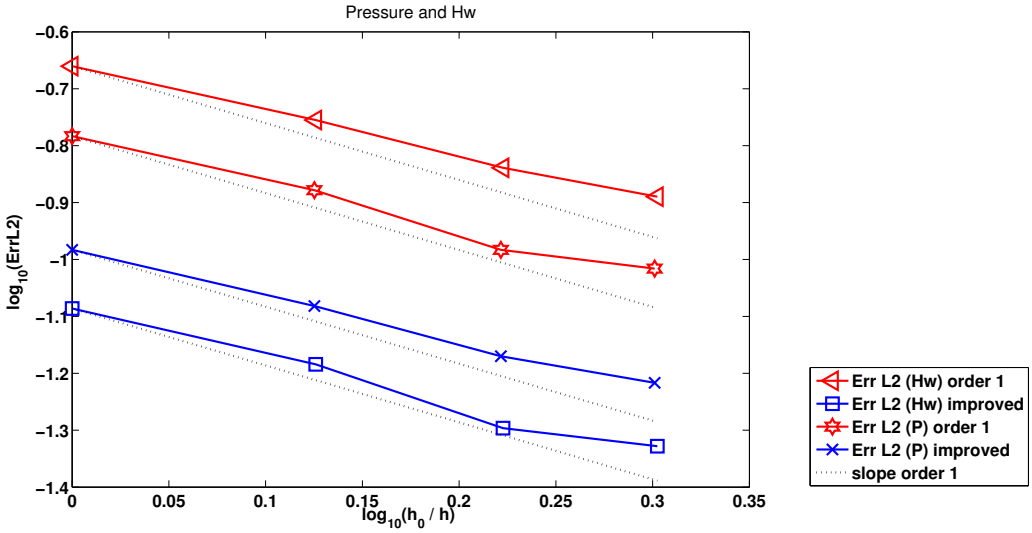

Figure 11: Convergence rate of the velocity

- DART-32401 localized at 260 NM West-southwest of Arica, Chile (Latitude/Longitude -20.473, -73.429), see Figure 12b,
- DART-32402 localized at 180 NM West of Caldera, Chile (Latitude/Longitude -26.743, -73.983), see Figure 12b.

To perform the simulation, we initialize the system on a square domain of size 2 200 km $\times$ 2 200 km, see Figures 12a and 12b. We simulate the seism by updating the topography data at the first time step. The displacement of the bottom is illustrated on Figure 13. In the simulation, the seism occurs at $t_1 = 0.2s$, namely the bottom topography is updated in one time step from its initial position to its final position at t_1. For the non-hydrostatic simulation, the mesh of the velocity has 451201 nodes which gives a size of edge's triangle of about 4 km, while the coarse mesh - on which the pressure is computed - has 113101 nodes. The hydrostatic simulation has been performed on the fine mesh. We use the improved order accuracy in time and space in the both simulations.

If we compare the simulated results obtained with the two models (hydrostatic and non-hydrostatic) together with the data obtained from the observation (given by the NOAA), we observe that the data are well recovered, especially for the first wave of the tsunami, see Figure 14a and **??**.

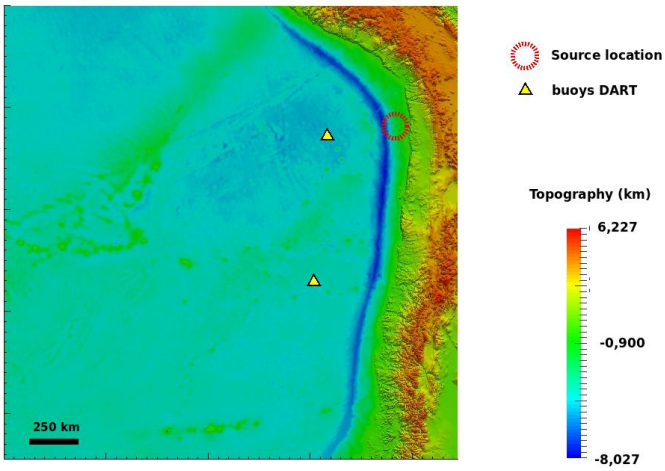

(a) Computational domain

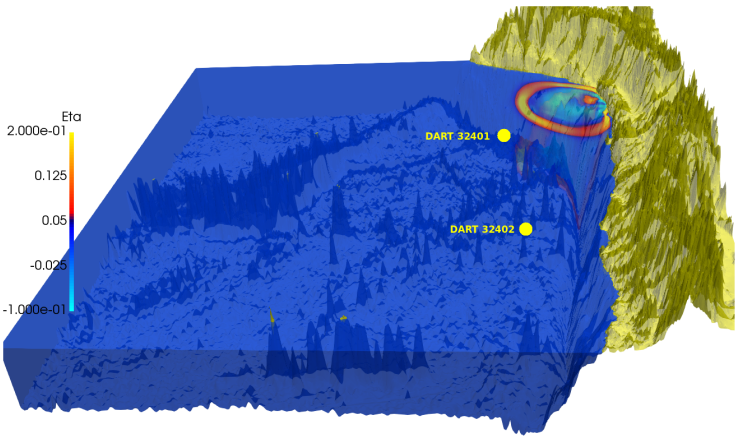

(b) DART buoys and variation of the free surface (m)

Figure 12: Chile domain and DART buoys localization.

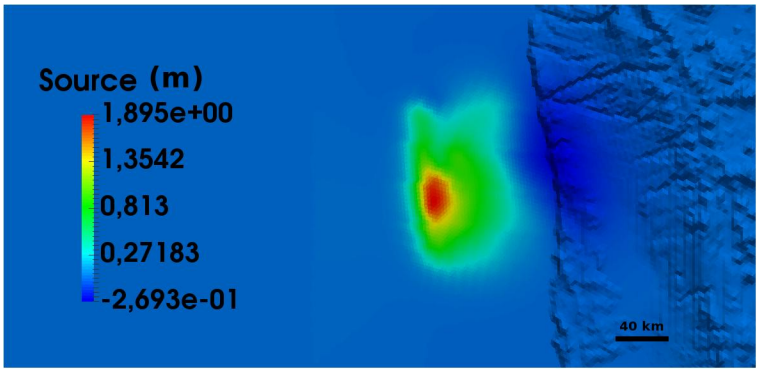

Figure 13: Source

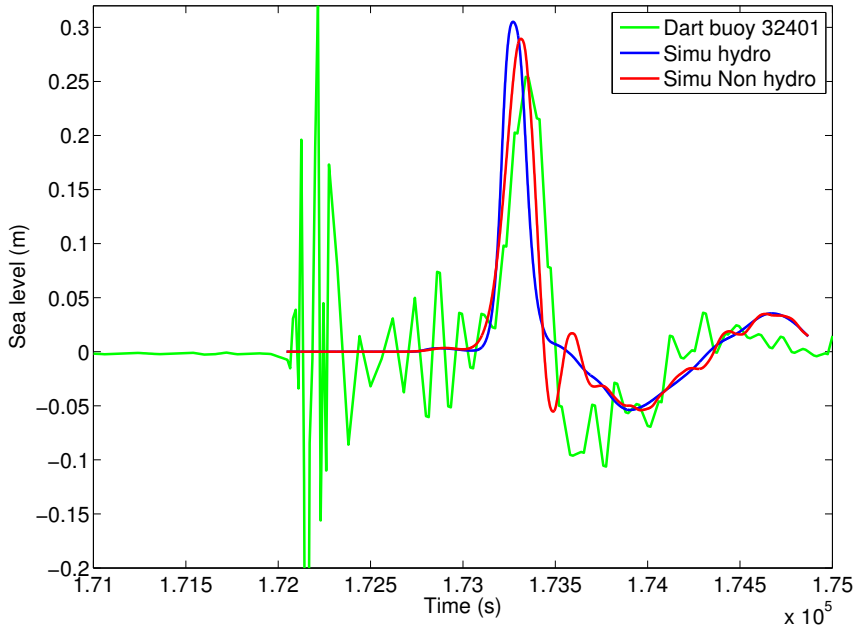

(a) Dart buoy 32401

Figure 14: Comparison between numerical results using both models (hydrostatic and non-hydrsotatic) and the data of the DART buoys.

9 Conclusion

In this paper, we have presented a new method for the two-dimensional dispersive shallow water system on unstructured meshes using a combined finite volume / finite element method. We have provided a numerical validation with two analytical solutions. The algorithm uses an iterative method of Uzawa type to solve the elliptic problem.
In a future work, we intend to optimize the computational cost in order to make the numerical method applicable to larger real domains, by focusing on the preconditioning of the iterative solver. Concerning the method, we would like to extend it to other dispersive models, in particular to a multilayer model.

Acknowledgments

The authors thank Robert Eymard and Martin Vallée for their helpful and constructive discussions that greatly contributed to improving the final version of the paper. The authors acknowledge the Inria Project Lab Algae in Silicio for its financial support. The first author received a partial grant from the Fondation Ledoux. This research is also supported by the ANR MIMOSA project.

References

[1] N. Aïssiouene. *Numerical analysis and discrete approximation of a dispersive shallow water model*. Theses, Pierre et Marie Curie, Paris VI, Dec. 2016.

[2] N. Aïssiouene, M.-O. Bristeau, E. Godlewski, and J. Sainte-Marie. A combined finite volume - finite element scheme for a dispersive shallow water system. *Networks and Heterogeneous Media*, 11(1):1–27, 2016.

[3] E. Audusse, F. Bouchut, M.-O. Bristeau, R. Klein, and B. Perthame. A fast and stable well-balanced scheme with hydrostatic reconstruction for Shallow Water flows. *SIAM J. Sci. Comput.*, 25(6):2050–2065, 2004.

[4] E. Audusse and M.-O. Bristeau. Transport of pollutant in shallow water flows : A two time steps kinetic method. *ESAIM: M2AN*, 37(2):389–416, 2003.

[5] E. Audusse and M.-O. Bristeau. A well-balanced positivity preserving second-order scheme for Shallow Water flows on unstructured meshes. *J. Comput. Phys.*, 206(1):311–333, 2005.

[6] E. Audusse and M.-O. Bristeau. Finite-volume solvers for a multilayer Saint-Venant system. *Int. J. Appl. Math. Comput. Sci.*, 17(3):311–319, 2007.

[7] E. Audusse, M.-O. Bristeau, and A. Decoene. Numerical simulations of 3d free surface flows by a multilayer Saint-Venant model. *Internat. J. Numer. Methods Fluids*, 56(3):331–350, 2008.

[8] E. Audusse, M.-O. Bristeau, and B. Perthame. Kinetic schemes for Saint-Venant equations with source terms on unstructured grids. Technical Report 3989, INRIA, Unité de recherche de Rocquencourt, FRANCE, 2000. http://www.inria.fr/rrrt/rr-3989.html.

[9] I. Babuska. The finite element method with lagrangian multipliers. *Numerische Mathematik*, 20:179–192, 1972/73.

[10] J. Behrens and F. Dias. New computational methods in tsunami science. *Philos Trans A Math Phys Eng Sci.*, Oct 28(373):(2053), 2015.

[11] P. Bonneton, E. Barthelemy, F. Chazel, R. Cienfuegos, D. Lannes, F. Marche, and M. Tissier. Recent advances in Serre-Green Naghdi modelling for wave transformation, breaking and runup processes. *European Journal of Mechanics - B/Fluids*, 30(6):589 – 597, 2011. Special Issue: Nearshore Hydrodynamics.

[12] F. Bouchut. *Nonlinear stability of finite volume methods for hyperbolic conservation laws and well-balanced schemes for sources.* Birkhäuser, 2004.

[13] F. Brezzi. On the existence, uniqueness and approximation of saddle-point problems arising from Lagrangian multipliers. *Rev. Française Automat. Informat. Recherche Opérationnelle Sér. Rouge*, 8(R-2):129–151, 1974.

[14] M.-O. Bristeau and B. Coussin. Boundary Conditions for the Shallow Water Equations solved by Kinetic Schemes. Rapport de recherche RR-4282, INRIA, 2001. Projet M3N.

[15] M.-O. Bristeau, A. Mangeney, J. Sainte-Marie, and N. Seguin. An energy-consistent depth-averaged Euler system: Derivation and properties. *Discrete and Continuous Dynamical Systems - Series B*, 20(4):961–988, 2015.

[16] F. Chazel, D. Lannes, and F. Marche. Numerical simulation of strongly nonlinear and dispersive waves using a Green–Naghdi model. *J. Sci. Comput.*, 48(1-3):105–116, July 2011.

[17] A. J. Chorin. Numerical solution of the Navier-Stokes equations. *Math. Comp.*, 22:745–762, 1968.

[18] R. Cienfuegos, E. Barthélemy, and P. Bonneton. A fourth-order compact finite volume scheme for fully nonlinear and weakly dispersive Boussinesq-type equations. Part I: Model development and analysis. *Internat. J. Numer. Methods Fluids*, 51(11):1217–1253, 2006.

[19] M.-W. Dingemans. *Wave propagation over uneven bottoms.* Advanced Series on Ocean Engineering - World Scientific, 1997.

[20] A. Duran and F. Marche. Discontinuous-Galerkin discretization of a new class of Green-Naghdi equations. *Communications in Computational Physics*, page 130, Oct. 2014.

[21] A. Duran and F. Marche. A discontinuous Galerkin method for a new class of Green-Naghdi equations on simplicial unstructured meshes. *ArXiv e-prints*, Apr. 2016.

[22] G. Ern. *Theory and Practice of Finite Elements*. Springer-Verlag New York, 2004.

[23] C. Escalante, T. Morales, and M.-J. Castro. Weakly dispersive shallow water flows: an efficient implementation using a finite-volume finite-difference scheme. In *Proceedings of the XXIV congress on differential equations and applications XIV congress on applied mathematics*, pages 255–259, Cadiz, 2015.

[24] S. Glimsdal, G. K. Pedersen, C. B. Harbitz, and F. Løvholt. Dispersion of tsunamis: does it really matter? *Natural Hazards and Earth System Sciences*, 13(6):1507–1526, 2013.

[25] E. Godlewski and P.-A. Raviart. *Numerical approximations of hyperbolic systems of conservation laws*. Applied Mathematical Sciences, vol. 118, Springer, New York, 1996.

[26] A. Green and P. Naghdi. A derivation of equations for wave propagation in water of variable depth. *J. Fluid Mech.*, 78:237–246, 1976.

[27] J.-L. Guermond. Some implementations of projection methods for Navier-Stokes equations. *ESAIM: Mathematical Modelling and Numerical Analysis*, 30(5):637–667, 1996.

[28] J.-L. Guermond and J. Shen. On the error estimates for the rotational pressure-correction projection methods. *Math. Comput.*, 73(248):1719–1737, 2004.

[29] F. Hecht and C. Pares. NSP1B3 : un logiciel pour resoudre les equations de Navier Stokes incompressible 3D. Research Report RR-1449, INRIA, 1991. Projet MENUSIN.

[30] O. Ladyzhenskaya. *The mathematical theory of viscous incompressible flow.* New York: Gordon and Breach, 1969.

[31] P. Lascaux and R. Theodor. *Analyse numérique matricielle appliquée à l'art de l'ingénieur*. Masson, 1986.

[32] O. Le Métayer, S. Gavrilyuk, and S. Hank. A numerical scheme for the Green-Naghdi model. *J. Comput. Phys.*, 229(6):2034–2045, 2010.

[33] C. Levermore and M. Sammartino. A shallow water model with eddy viscosity for basins with varying bottom topography. *Nonlinearity*, 14(6):1493–1515, 2001.

[34] O. Pironneau. *Méthodes des éléments finis pour les fluides.* Masson, 1988.

[35] R. Rannacher. On Chorin's projection method for the incompressible Navier-Stokes equations. In G. Heywood, John, K. Masuda, R. Rautmann, and A. Solonnikov, Vsevolod, editors, *The Navier-Stokes Equations II — Theory and Numerical Methods*, volume 1530 of *Lecture Notes in Mathematics*, pages 167–183. Springer Berlin Heidelberg, 1992.

[36] J. Sainte-Marie. Vertically averaged models for the free surface Euler system. Derivation and kinetic interpretation. *Math. Models Methods Appl. Sci. (M3AS)*, 21(3):459–490, 2011.

[37] W. C. Thacker. Some exact solutions to the non-linear shallow-water wave equations. *J. Fluid Mech.*, 107:499–508, 1981.

[38] M. Vallée, R. Grandin, S. Ruiz, B. Delouis, C. Vigny, E. Rivera, E.-M. Aissaoui, S. Allgeyer, Q. Blétery, C. Satriano, N. Poiata, P. Bernard, J.-P. Vilotte, and B. Schurr. Complex rupture of an apparently simple asperity during the 2014/04/01 Pisagua earthquake (Northern Chile, Mw=8.1). In *EGU General Assembly Conference Abstracts*, volume 18 of *EGU General Assembly Conference Abstracts*, page 8660, Apr. 2016.